PROCEEDINGS

MMM 2008

Fourth International Conference

MULTISCALE MATERIALS MODELING

OCTOBER 27-31, 2008 ▪ TALLAHASSEE, FLORIDA, USA

Tackling Materials Complexities via Computational Science

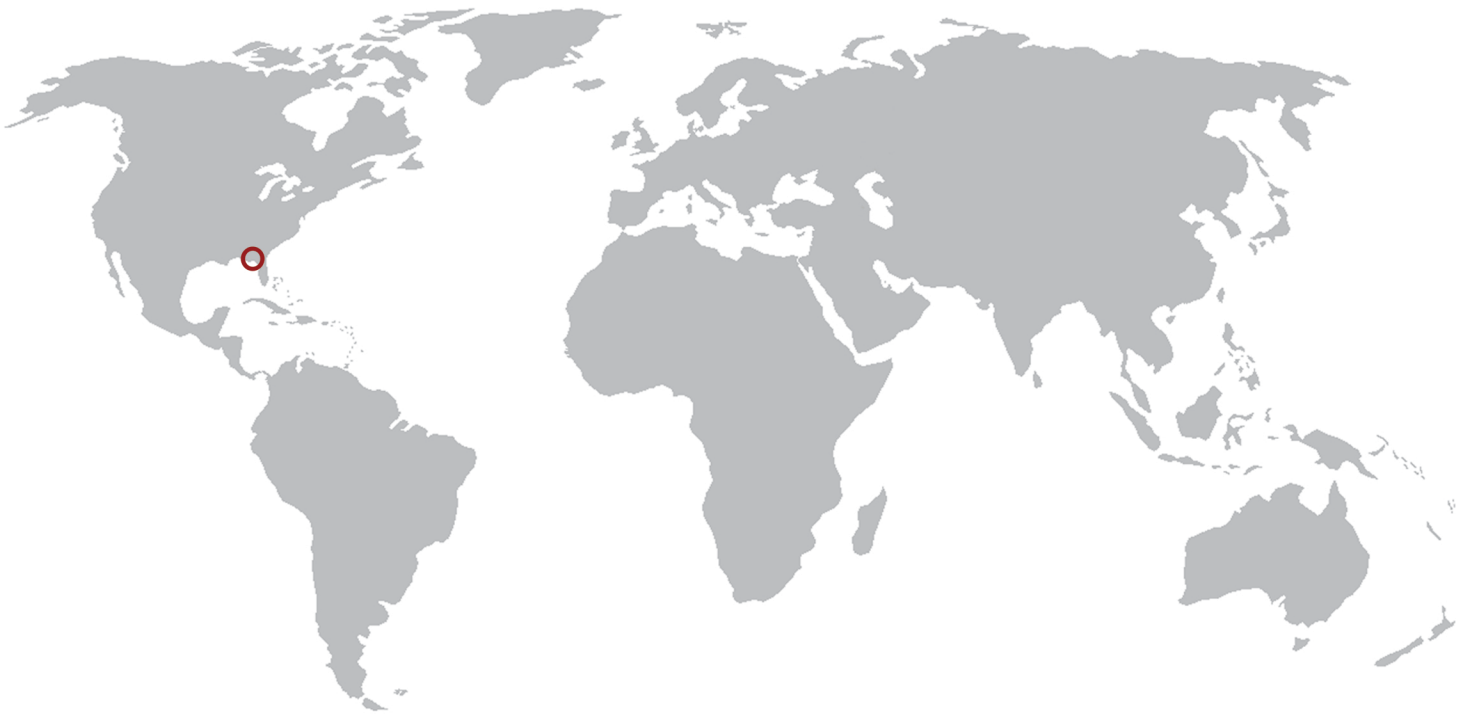

Hosted by the Department of Scientific Computing and Florida State University

DEPARTMENT OF Scientific COMPUTING

FLORIDA STATE UNIVERSITY 1851 VIRES ARTES MORES

Proceedings of

MMM 2008

Fourth International Conference

MULTISCALE MATERIALS MODELING

OCTOBER 27-31, 2008 ▪ TALLAHASSEE, FLORIDA, USA

Anter El-Azab
Editor

Organized and Hosted by
The Department of Scientific Computing and
Florida State University

DEPARTMENT OF Scientific COMPUTING

Papers published in this volume constitute the proceedings of the Fourth International Conference on Multiscale Materials Modeling (MMM-2008). Papers were selected by the program committee for oral or poster presentation. They are published as submitted, in the interest of timely dissemination.

ISBN 978-0-615-24781-6

Department of Scientific Computing
Florida State University
400 Dirac Science Library
P.O. Box 3064120
Tallahassee, FL 32306-4120

Printed in the United States of America

Forward

The field of multiscale modeling of materials promotes the development of predictive materials research tools that can be used to understand the structure and properties of materials at all scales and help us process materials with novel properties. By its very nature, this field transcends the boundaries between materials science, mechanics, and physics and chemistry of materials. The increasing interest in this field by mathematicians and computational scientists is creating opportunities for solving computational problems in the field with unprecedented levels of rigor and accuracy. Because it is a part of the wider field of materials science, multiscale materials research is intimately linked with experiments and, together, these methodologies serve the dual role of enhancing our fundamental understanding of materials and enabling materials design for improved performance.

The increasing role of multiscale modeling in materials research motivated the materials science community to start the Multiscale Materials Modeling (MMM) Conference series in 2002, with the goal of promoting new concepts in the field and fostering technical exchange within the community. Three successful conferences in this series have been already held:

- The First International Conference on Multiscale Materials Modeling (MMM-2002) at Queen Mary University of London, UK, June 17-20, 2002,
- Second International Conference on Multiscale Materials Modeling (MMM-2004) at the University of California in Los Angeles, USA, October 11-15, 2004, and
- Third International Conference on Multiscale Materials Modeling (MMM-2006) at the University of Freiburg, Germany, September 18-22, 2006.

The Fourth International Conference on Multiscale Materials Modeling (MMM-2008) held at Florida State University comes at a time when the wider computational science field is shaping up and the synergy between the materials modeling community and computational scientists and mathematicians is becoming significant. The overarching theme of the MMM-2008 conference is thus chosen to be "*Tackling Materials Complexities via Computational Science*," a theme that highlights the connection between multiscale materials modeling and the wider computational science field and also reflects the level of maturity that the field of multiscale materials research has come to. The conference covers topics ranging from basic multiscale modeling principles all the way to computational materials design. Nine symposia have been organized, which span the following topical areas:

- Mathematical basis for multiscale modeling of materials
- Statistical frameworks for multiscale materials modeling
- Mechanics of materials across time and length scales
- Multiscale modeling of microstructure evolution in materials
- Defects in materials
- Computational materials design based on multiscale and multi-level modeling principles

- Multiscale modeling of radiation effects in materials and materials response under extreme conditions
- Multiscale modeling of bio and soft matter systems

The first five topical areas are intended to cover the theoretical and computational basis for multiscale modeling of materials. The sixth topical area is intended to demonstrate the technological importance and industrial potential of multiscale materials modeling techniques, and to stimulate academia-laboratory-industrial interactions. The last two topical areas highly overlap with the earlier ones, yet they bring to the conference distinct materials phenomena and modeling problems and approaches with unique multiscale modeling aspects.

This conference would not have been possible without the help of many individuals both at Florida State University and around the world. Of those, I would like to thank the organizing team of MMM-2006, especially Professor Peter Gumbsch, for sharing their experience and much organizational material with us. I also thank all members of the International Advisory Board for their support and insight during the early organizational phase of the conference, and the members of the International Organizing Committee for the hard work in pulling the conference symposia together and for putting up with the many organization-related requests. Thanks are due to Professor Max Gunzburger, Chairman of the Department of Scientific Computing (formerly School of Computational Science) and to Florida State University for making available financial, logistical and administrative support without which the MMM-2008 would not have been possible. The following local organizing team members have devoted significant effort and time to MMM-2008 organization: Bill Burgess, Anne Johnson, Michele Locke, Jim Wilgenbusch, Christopher Cprek and Michael McDonald. Thanks are also due to my students Srujan Rokkam, Steve Henke, Jie Deng, Santosh Dubey, Mamdouh Mohamed and Jennifer Murray for helping with various organizational tasks. Special thanks are due to Bill Burgess and Srujan Rokkam for their hard work on the preparation of the proceedings volume and conference program.

I would like to thank the MMM-2008 sponsors: Lawrence Livermore National Laboratory (Dr. Tomas Diaz de la Rubia), Oak Ridge National Laboratory (Dr. Steve Zinkle) and Army Research Office (Drs. Bruce LaMattina and A.M. Rajendran) for the generous financial support, and thank TMS (Dr. Todd Osman) for the sponsorship of MMM-2008 and for advertising the conference through the TMS website and other TMS forums.

I would also like to thank all plenary speakers and panelists for accepting our invitation to give plenary lectures and/or serve on the conference panels. Lastly, I would like to thank the session chairs for managing the conference sessions.

Anter El-Azab
Conference Chair

International Advisory Board

Dr. Tomas Diaz de la Rubia	LLNL, USA
Prof. Peter Gumbsch	Fraunhofer Institute IWM, Freiburg, Germany
Dr. A.M. Rajendran	ARO, USA
Dr. Steve Zinkle	ORNL, USA
Prof. Anter El-Azab	FSU, USA
Prof. Michael Zaiser	Edinburgh, UK
Prof. Xiao Guo	Queens, London, UK
Prof. Shuichi Iwata	University of Tokyo, Japan
Prof. Jan Kratochvil	CTU, Prague, Czech Republic
Prof. Nasr Ghoniem (Chair)	UCLA, USA
Dr. Ladislas Kubin	ONERA-LEM, France
Prof. Shaker Meguid	Toronto, Canada
Prof. Alan Needleman	Brown, USA
Prof. Michael Ortiz	Caltech, USA
Prof. David Pettifor	Oxford, UK
Prof. Robert Phillips	Caltech, USA
Prof. Dierk Raabe	Max Planck Institute, Duesseldorf, Germany
Prof. Yoji Shibutani	Osaka University, Japan
Prof. Subra Suresh	MIT, Massachusetts USA
Prof. Yoshihiro Tomita	Kobe University, Japan
Prof. Erik Van der Giessen	University of Groningen, The Netherlands
Dr. Dieter Wolf	INL, USA
Prof. Sidney Yip	MIT, USA
Prof. David Bacon	Liverpool, UK
Dr. Michael Baskes	LANL, USA
Prof. Esteban Busso	Ecole des Mines, France
Prof. Timothy Cale	RPI, New York, USA
Dr. Moe Khaleel	PNNL, USA
Prof. David Srolovitz	Yeshiva, USA
Prof. Emily Carter	Priceton University, USA
Dr. Dennis Dimiduk	AFRL, USA
Prof. Rich Le Sar	Iowa State University, USA

International Organizing Committee

Weinan E	Princeton University, USA
Max Gunzburger	Florida State University, USA
Mitchell Luskin	University of Minnesota, USA
Rich Lehoucq	Sandia National Laboratories, USA
A.M. Rajendran	U.S. Army Research Office, USA
Stefano Zapperi	University of Rome, Italy
M.-Carmen Miguel	University of Barcelona, Spain
Mikko Alava	Helsinki University of Technology, Finland
Istevan Groma	Eötvös University, Hungary
Tom Arsenlis	Lawrence Livermore National Laboratory, USA
Peter Chung	Army Research Laboratory, USA

Marc Geers	Eindhoven University of Technology, The Netherlands
Yoji Shibutani	Osaka University, Japan
Dieter Wolf	Idaho National Laboratory, USA
Jeff Simmons	Air Force Research Laboratory, USA
Simon Phillpot	University of Florida, USA
Anter El-Azab (Chair)	Florida State University, USA
Daniel Weygand	University of Karlsruhe (TH), Germany
Zi-Kui Liu	Pennsylvania State University, USA
Hamid Garmestani	Georgia Institute of Technology, USA
Moe Khaleel	Pcific Northwest National Laboratory, USA
Mei Li	Ford Motor Company, USA
Fie Gao	Pacific Northwest National Laboratory, USA
Roger Stoller	Oak Ridge National Laboratory, USA
Pascal Bellon	University of Illinois, Urbana-Champaign, USA
Syo Matsumura	Kyushu University, Japan
Jeffery G. Saven	University of Pennsylvania, USA
Wei Yang	Florida State University, USA
T.P. Straatsma	Pacific Northwest National Laboratory, USA
L.P. Kubin	CNRS-ONERA, France
S.J. Zinkle	Oak Ridge National Laboratory, USA
Jaafar El-Awady	University of California, Los Angeles, USA
Shahram Sharafat	University of California, Los Angeles, USA
Hanchen Huang	Rensselaer Polytechnic Institute, USA
Yury N. Osetskiy	Oak Ridge National Laboratory, USA
Ron O. Scattergood	North Carolina State University, USA
Anna M. Serra	Universitat Politecnica de Catalunya, Spain

Local Organizing Committee (Florida State University, USA)

Prof. Anter El-Azab (Chair)
Prof. Max Gunzburger (Co-Chair)
Anne Johnson (Public relations and marketing)
Bill Burgers (Graphics and publications)
Srujan Rokkam (Proceedings and printing)
Michael McDonald (Webmaster)
Michele Locke (Finances)

Sponsors

Special thanks to the following sponsors:

- The Army Research Office
- Lawrence Livermore National Laboratory
- Oak Ridge National Laboratory

for their generous financial support, and to

- The Minerals, Metals & Materials Society (TMS)

for the sponsoring and advertising the conference through the TMS website.

Contents

Symposium 9

Molecular Simulations: Pb Segregation to Grain Boundaries and Effects on Deformation in Nanocrystalline Al. 795
R. Scattergood, S. Jang, Y. Purohit, D. Irving, D. Brenner
Session M-B

Modeling of Plastic Deformation of Non-magnetic Transition Body-Centered-Cubic Metals: From Atomic to Continuum Level 796
V. Vitek, R. Gröger
Session M-B

Dislocation Dynamics and Plasticity in Martensitic Transformations 797
R. C. Pond, J. P. Hirth
Session M-B

Atomic Simulation of Twin Boundaries in HCP Metals: Mobility and Defect Interaction 803
A. Serra, D. J. Bacon
Session M-B

Dislocation activity within nanocrystalline metals: A molecular dynamics study 807
C. Brandl, E. Bitzek, P. M. Derlet, H. Van Swygenhoven
Session M-B

Dynamic observations of heavy-ion damage in Fe and Fe-Cr Alloys
M L Jenkins, Z. Yao, S. Xu, M. Hernandez-Mayoral, M. Kirk
Session M-C

Molecular Ion Irradiations of Molybdenum 813
C A English, M L Jenkins
Session M-C

Atomic-scale Modeling of Helium Atoms and Vacancies in Dislocations in alpha-Iron 814
H. Heinisch
Session T-D

Atomic-Level Modeling of Migration of Vacancies, He Interstitials, and Nucleation of He-V clusters at Grain Boundaries in alpha-Fe 815
F. Gao
Session T-D

Resistance to Fast Dislocation Motion 816
C. H. Woo
Session T-D

Hardening by completely and partially absorbed ½<111> and <100> dislocation loops reacting with dislocations in α-Fe 817
D. Terentyev, D.J. Bacon, P. Grammatikopoulos, Yu.N. Osetsky
Session W-C

Determination of the Activation Energy of Dislocation-defect Interactions in Molecular Dynamics Simulations 823
G. Monnet, Y. Osetsky, D. J. Bacon
Session W-C

Molecular Dynamic Study of Screw Dislocation – Irradiation Defect Interactions 824
C. Domain, G. Monnet
Session W-C

Object kinetic Monte Carlo study of the sink strength of dislocations 825
L. Malerba, C. Becquart, C. Domain
Session W-C

A modelling study of the relationship between primary damage features and the long term defects clusters growth 829
M. Hou, A. Souidi, C. S. Becquart, C. Domain, L. Malerba
Session W-C

On the role of helical turns in the formation of clear bands in irradiated materials 830
D. Rodney, T. Nogaret, M. Fivel
Session W-D

Dynamics of dislocation-localized obstacle interaction: what can we learn from atomic level modelling 831
Y. Osetsky
Session W-D

Dislocation interaction with C in alpha-Fe: a comparison between Atomic simulations and elasticity theory 832
E. Clouet, S. Garruchet, H. Nguyen, M. Perez, C. Becquart
Session W-D

Computer Simulation of Effects of PKA Nature on Cascade Damage in Iron 833
A. Calder, D. Bacon, S. Barashev, Y. Osetsky
Session Th-C

Defect Production in Iron: Review of Atomistic Simulations 834
R. E. Stoller
Session Th-C

Decoration of Edge Dislocation with Interstitial Clusters Under Neutron Irradiation 835
A. V. Barashev, S. I. Golubov, D. J. Bacon,
Y. N. Osetsky, R. E. Stoller
Session Th-C

Point defects in Zirconium and their influence on radiation damage 836
P. Gasca, C. Domain, A. Legris
Session Th-C

Core Structure, Peierls Potential and Kinks of Screw Dislocations in Iron from First Principles 837
L. Ventelon, F. Willaime, E. Clouet
Session Th-C

Mechanisms Operating during Plastic Deformation of Metals 838
H. Trinkaus, B.N. Singh, S.I. Golubov
Session Th-D

On the role of elastic strains in the precipitation of second phases 839
V. Mohles, E. Jannot, G. Gottstein
Session Th-D

Substitutional Al solute interaction with edge and screw dislocation in Ni: a comparison between atomistic computation and continuum elastic theory 840
S. Patinet
Session Th-D

Influence of inertial effects on the motion and the interaction of dislocations 844
L. Pillon, C. Denoual, Y.-P. Pellegrini
Session Th-D

Symposium 9

Elasticity to atomistics: predictive modeling of defect behavior

Honoring Professor David J. Bacon on the occasion of his retirement from the University of Liverpool

Molecular Simulations: Pb Segregation to Grain Boundaries and Effects on Deformation in Nanocrystalline Al.

Ronald Scattergood[1], Seonhee Jang[2], Yojna Purohit[1], Douglas Irving[1], Donald Brenner[1]

[1]Department of Materials Science & Engineering, NC State University, Campus Box 7907, Raleigh, NC 27695-7907, (E-mails: scatterg@ncsu.edu, yojna28@gmail.com, dlirving@ncsu.edu, brenner@ncsu.edu)
[2]Samsung Semiconductor (E-mail: Seonhee.Jang@gmail.com)

ABSTRACT

The energies for symmetric tilt grain boundaries in pure Al and in Al with Pb atoms at coincident sites along the grain boundaries were obtained using a modified embedded atom method potential and density functional theory. The analytic potential and first principles calculations predict that Pb segregation to the grain boundaries is energetically preferred compared to the dilute solution. A reduction of grain boundary energy with an increasing number of Pb atoms on the grain boundary was predicted by our calculations, with a negative energy with respect to the ideal dilute solid solution predicted when more than 50 percent of the coincident sites per unit grain boundary area are replaced by Pb atoms. A disclination model was proposed to calculate the grain boundary energy over the entire range of tilt angles. In conjunction with these studies, straining simulations using a 2D columnar model were done for 10 nm grain-size pure Al and Al containing 1, 2 and 3 at% Pb segregated on the grain boundaries. Nucleation of partial dislocations and twins during straining was suppressed when at% Pb increased, and the yield stress decreased. Grain boundaries with Pb segregates were very robust against dissociation during straining compared to pure Al. These observations are discussed in terms of Pb segregation on grain boundaries and the concomitant transition of plastic straining from intra-grain dislocation mechanisms to inter-grain shear mechanisms.

Modeling of Plastic Deformation of Non-magnetic Transition Body-Centered-Cubic Metals: From Atomic to Continuum Level

V. Vitek[1*] and R. Gröger[2]

[1]Department of Materials Science and Engineering, University of Pennsylvania, Philadelphia, PA 19104, USA
[2]Los Alamos National Laboratory, Theoretical Division, Los Alamos, NM 87545, USA
(E-mail: [*]vitek@seas.upenn.edu)

ABSTRACT

It is well established that 1/2⟨111⟩ screw dislocations in BCC metals possess non-planar cores and therefore a very high Peierls stress and, consequently, control the plastic behavior of these metals. This is the reason why the atomic structure of screw dislocations in BCC metals has been investigated extensively over many years. In this presentation we first present results of the recent molecular statics calculations of the structure and glide of 1/2⟨111⟩ screw dislocations in several transition metals, performed using the recently developed bond-order potentials that reflect the mixed nearly free electron and covalent bonding. The most important finding of these calculations is a complex dependence of the Peierls stress on the applied stress tensor, in particular its dependence on both shear stresses parallel and perpendicular to the Burgers vector. Based on the results of these atomistic studies we formulate a general yield criterion for the *non-associated flow* that includes the effect of the full stress tensor and not only the so called Schmid stress, i. e. the stress in the slip direction in the slip plane. This criterion is then applied when analyzing deformation of single crystals in the framework of crystal plasticity. Using this criterion we demonstrate how the yield surfaces differ significantly from those based on the Tresca criterion that relates to the Schmid law and also how they vary from one transition metal to another. The latter is directly related to subtle differences in the interatomic bonding in different transition metals. This theoretical development also allows linking atomic level calculations with experimental studies of deformation of single crystals. As an example we show how the observed characteristics of the low temperature yielding in molybdenum, in particular the tension-compression asymmetry, can be understood in this framework.

This research was supported by the U.S. Department of Energy, BES Grant no. DE-PG02-98ER45702.

Dislocation Dynamics and Plasticity in Martensitic Transformations

R. C. Pond[1] and J. P. Hirth[2]

[1]School of Engineering, Computing and Mathematics, University of Exeter, U.K.
(E-mail: r.c.pond@exeter.ac.uk)
[2]114 E. Ramsey Canyon Road, Hereford, AZ 85615, USA.
(E-mail: jphmdh@cox.net)

ABSTRACT

A physical model of the structure of parent-martensite interfaces has been developed based on dislocation theory and topological arguments. Two arrays of defects are generally present in the habit plane; one is an array of disconnections (line defects with dislocation and step character, also known as transformation dislocations), and the other is produced by crystal defects (slip or twinning) in the martensite crystal. The geometry of the defect network determines the transformation crystallography. It is shown explicitly that the mechanism of interface motion, lateral motion of disconnections across the interface, is conservative. The object of the present paper is to discuss the mobility of such defect networks in response to the wide range of driving forces encountered in martensitic transformations, and the plastic deformation induced. It is important to distinguish between the plasticity induced by motion of the defect network and the distortions arising due to the elastic fields of the defects in the static state. The former can be represented as an engineering strain expressed in terms of the Burgers vectors of the crystal defects and disconnections and their planes of motion. The latter include short-range coherency strains and small ancillary rotations that modify the orientation relationship of the parent/martensite crystals.

1. Introduction

The Phenomenological Theory of Martensite Crystallography (PTMC) ([1], [2]) has been used to predict the habit plane (HP), orientation relationship (OR) and transformation displacement (TD) in a wide range of cases. This success implies that the PTMC's underlying hypothesis, i.e. that the HP is an invariant plane of the shape transformation, is a sufficient criterion for predicting interfaces with no long-range distortion field. Further progress in our understanding of martensitic transformations requires a physical model, incorporating the transformation mechanism itself. Such an approach could elucidate the reasons why application of the PTMC is unsatisfactory for certain transformations [3]. Also, a physical model would enable quantitative determination of interfacial energies and transformation rates. The objective of the current paper is to outline a physical model based on dislocation theory, named the Topological Model (TM) [4,5].

2. Topological Model

The foundation of the TM is to identify a low-energy interface, separating parent from product, which produces the transformation strain by migrating without concomitant

long-range diffusion. Such interfaces are partially coherent and have the general form illustrated in Fig 1; coherent terraces are reticulated by a network of dislocations and disconnections (transformation dislocations). The former are perfect, partial or twinning dislocations emanating from the product crystal, and are designated Lattice-Invariant Deformation (LID) in the PTMC. These have Burgers vector $\mathbf{b}^L$, line sense ξ^L and spacing d^L. The latter have both dislocation and step character (with height h [5]), and are defined by $(\mathbf{b}^D, h)$, ξ^D and d^D. Two purposes are fulfilled by the defect network; it accommodates coherency strains, and lateral motion of the disconnections produces coupled migration and displacement. Similar models of martensitic interfaces have been discussed in the literature for some time ([4], [5]), and these ideas are formally and rigorously set out in the TM. The following elements of the TM are noteworthy and discussed briefly below: the significance of coherent terraces, definition of $(\mathbf{b}^D, h)$, determination of network parameters $\mathbf{b}^L, \xi^L, d^L$, $(\mathbf{b}^D, h)$, ξ^D and d^D, and determination of the transformation crystallography (HP, OR, TD).

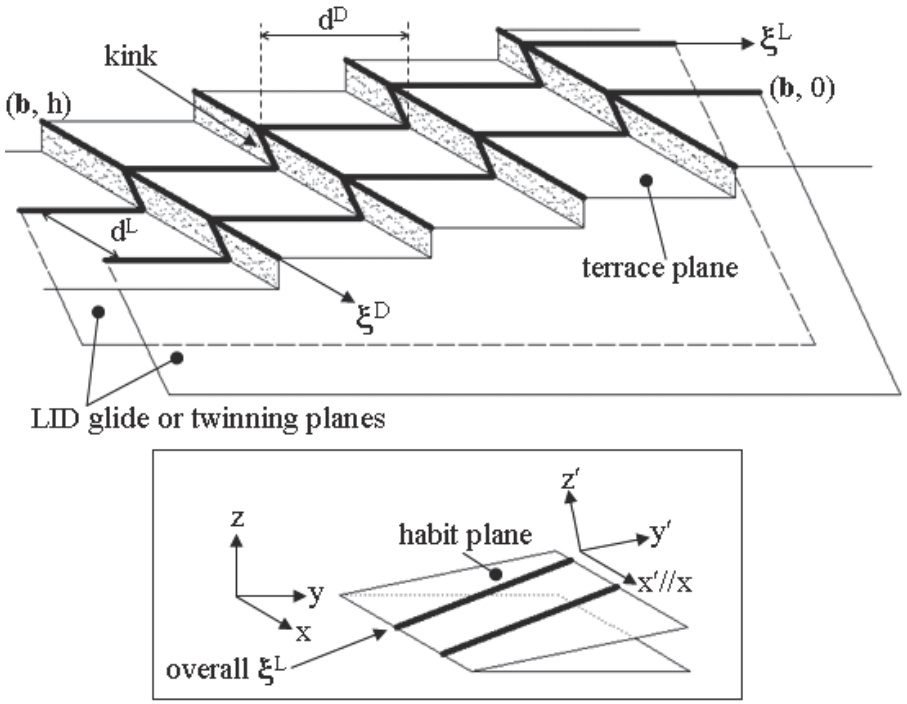

Figure 1. Schematic illustration of an interphase interface showing the terrace segments and defect arrays. Coherently strained terraces are reticulated by arrays of disconnections (**b**, h) with spacing d^D and crystal slip dislocations (**b**, 0) in the (lower) μ crystal. The terrace and habit (primed) coordinate frames are shown and the line directions of the disconnections, ξ^D, and dislocations, ξ^L, are parallel to x and close to y' respectively.

Coherent terraces are central to the TM, firstly because they exhibit pronounced energy minima ([6], [7]). Secondly, conservative motion of disconnections across interphase interfaces only arises on such terraces [8]. In this case, passage of a disconnection relocates atoms from parent sites to product sites by a combination of shear and shuffle, thereby conserving the number of substitutional sites but, in general, changing the volume occupied by them according to the difference in density

of the two phases. Crystal dislocations (LID) do not move laterally along the interface in the TM, but are assumed to glide through the martensite in the wake of a moving interface; consequently, their **b** must be inclined to the HP.

For quantitative modelling it is essential to be precise about the definition of $\mathbf{b}^L$ and $(\mathbf{b}^D, h)$, and this is achieved using the Topological Theory of Interfacial Defects [9]. This rigorous theory is expressed in terms of the space-group symmetries of the two crystals; it does not require the creation of a lattice common to both crystals, as in the CSL and DSC approach.

Line directions and spacings of candidate dislocation/disconnection networks to accommodate coherency strains can be determined using the Frank-Bilby equation [10, 11]. However, the step character of disconnections introduces an additional topological factor to be taken into account. Dislocation content is now coupled to the orientation of the interface plane, and an iterative procedure is needed to find the network that relieves coherency strains on the resulting habit plane (as opposed to the terrace plane).

As is apparent in Fig 1, the HP deviates from the terrace plane to an extent dependent on ξ^D and d^D (the terrace and habit coordinate frames are designated x, y, z and x', y', z' respectively). Also, the OR of the adjacent crystals is not determined exclusively by the crystal alignment across the coherent terrace. According to the topological model, the distortion field of a static interface can be written as the sum of a tensor strain and a rotation

$$\Gamma^s(x', y', z') = \begin{pmatrix} \varepsilon'_{xx} & \varepsilon'_{xy} & \varepsilon'_{xz} \\ \varepsilon'_{xy} & \varepsilon'_{yy} & \varepsilon'_{yz} \\ \varepsilon'_{xz} & \varepsilon'_{yz} & \varepsilon'_{zz} \end{pmatrix} + \begin{pmatrix} 0 & -\phi'_{xy} & \phi'_{xz} \\ \phi'_{xy} & 0 & -\phi'_{yx} \\ -\phi'_{xz} & \phi'_{yz} & 0 \end{pmatrix}. \quad (1)$$

The strain and rotational distortion components of $\Gamma^s(x', y', z')$ vary from point to point, describing both the short- and long-range fields produced by superposition of the coherency strain and the elastic field of the defect network. At short-range all strains are partitioned between the phases in a manner depending on their relative elastic compliances. In the case where the coherency strain is completely accommodated by the network, all component strains except ε'_{zz} vanish at long-range. At short-range, these strains alternate in sign along x' and y' respectively, in anti-phase across the habit plane, and diminish to zero when $z' \approx z_d$ is approximately equal to the relevant defect spacing, d^D or d^L [12]. The magnitude of ε'_{zz} will be finite at long-range in the "single interface" case, where no constraint by the matrix is present. For $z' > z_d$ the rotational distortions are constant and equal to the ancillary tilts, ϕ'_{xz} and ϕ'_{yz}, and twist, ϕ'_{xy}.

Moving disconnections serve to produce the plastic transformation strain. A moving dislocation sweeping an area **A** produces an engineering strain per unit volume $\mathbf{\Gamma} = \mathbf{bA^t}$. Here, $\mathbf{A} = A\mathbf{n}$ with **n** a unit normal to **A**, and the superscript indicates a row vector. Hence a straight disconnection of length ℓ moving by δy in the y direction in the terrace plane coordinates sweeps an area $A = \ell \delta y$, numerically equal to δy for a defect of unit length. This motion produces an engineering strain

$$\mathbf{\Gamma} = \begin{pmatrix} 0 & 0 & \gamma_{xz} \\ 0 & 0 & \gamma_{yz} \\ 0 & 0 & \varepsilon_{zz} \end{pmatrix} = \delta y \begin{pmatrix} b_x \\ b_y \\ b_z \end{pmatrix}^D \begin{pmatrix} 0 & 0 & n_z \end{pmatrix}, \tag{2}$$

with $n_z = 1$. Here b_y and b_z are edge components and b_x is the screw component of a disconnection with ξ^D parallel to x/x'. This strain matrix can also be regarded as a tensor strain $\mathbf{E}_t$ plus a rotation $\mathbf{R}$

$$\Gamma = \mathbf{E}_t + \mathbf{R} = \begin{pmatrix} 0 & 0 & \varepsilon_{xz} \\ 0 & 0 & \varepsilon_{yz} \\ \varepsilon_{xz} & \varepsilon_{yz} & \varepsilon_{zz} \end{pmatrix} + \begin{pmatrix} 0 & 0 & \phi_{xz} \\ 0 & 0 & -\phi_{yz} \\ -\phi_{xz} & \phi_{yz} & 0 \end{pmatrix} = \delta y \begin{pmatrix} b_x \\ b_y \\ b_z \end{pmatrix}_D \begin{pmatrix} 0 & 0 & n_z \end{pmatrix}. \tag{3}$$

Near a single disconnection there can also be strains ε_{xy}, arising from the screw component, if present. However the strain is very small or zero on the terrace plane, and is cancelled by the fields of other disconnections in the array when $z > \sim d^D$ and therefore is ignored as a local effect. Here, for example, the component $\varepsilon_{xz} = \gamma_{xz}/2 = b_x\delta y/2$ and $\varphi_{xz} = b_x\delta y/2$. For a train of disconnections as in figure 1, with $1/d^D$ defects per unit length in the y direction, the strain produced by the train is Γ / d^D. Uniform motion of unit area of the train by $-\delta y$ transforms a volume numerically equal to $h\delta y / d^D$ from λ to μ and translates the habit plane in the z' direction by $\delta z' = -\delta y \sin\theta$. Thus, knowing **b,** one can simply write the total engineering strain components produced by motion of the disconnection train, Γ_m^D, as

$$\Gamma_m^D = \begin{pmatrix} 0 & 0 & \gamma_{xz} \\ 0 & 0 & \gamma_{yz} \\ 0 & 0 & \varepsilon_{zz} \end{pmatrix} = \frac{\delta y}{d^D} \begin{pmatrix} b_x \\ b_y \\ b_z \end{pmatrix}^D \begin{pmatrix} 0 & 0 & n_z \end{pmatrix}. \tag{4}$$

We emphasize that these are plastic strains and rotations. There are also rotations associated with the elastic distortion fields of the defects as discussed in Section 2; these are associated with the interface structure, which is unchanged on average as the train of defects moves. Thus the rotations connected to the elastic distortions are unchanged by the motion δz' of the habit plane. The LID defects are also associated with the interface structure and have long-range rotations which are also unchanged by the motion δz' of the habit plane. The LID defects that are translated in the z-direction by the disconnection motion produce an additional plastic engineering strain

$$\Gamma_m^L = \frac{\delta y}{d^L \cos\chi} \begin{pmatrix} b_x \\ b_y \\ b_z \end{pmatrix}^L \begin{pmatrix} g_x & g_y & g_z \end{pmatrix}, \tag{5}$$

where $[g_x, g_y, g_z]$ is the unit normal of the glide/twinning plane and χ is the angle between the glide and terrace planes.

We now summarize the implementation of the topological model to find the defect structure of a two-dimensional transformation interface; full details have been

presented elsewhere [5]. One first seeks a matched terrace plane with small misfit; these display energy minima, and, as outlined above, are essential for diffusionless transformations. Then the crystals adjoining the terrace plane are uniformly strained to achieve coherence at the interface. The crystal lattices are interpenetrated to form a dichromatic pattern. This is the coherent reference state. Inspection of the reference state allows one to select candidate disconnections (**b**, h) and dislocations (**b**, 0). For simple systems, one can then deduce the correct network parameters to relieve all long-range coherency strains, and thus determine the orientation of the habit plane and the ancillary rotation. For less simple systems one can proceed to solve the Frank-Bilby equation iteratively to determine the spacings and line directions. In any case, tilt or twist rotations can be superposed if needed, partitioning the rotations between the two crystals.

3.1 Disconnection motion

The nucleation of a new plate of martensite is clearly heterogeneous, with the possible exception of driving forces so large that the mechanism approaches one akin to spinodal decomposition, a case not considered here that may even occur by direct shuffling rather than defect motion. Once nucleated, there are several sources for continued formation of disconnections at a source. These include pole-type spiral mechanisms, strain fields at plate facets, precipitate intersections [83], and repeated nucleation from grain boundaries. Hence, transformation proceeds by a train of moving disconnections. There are three classes of behaviour. For fast martensite, such as that forming in quenched steels, the driving forces are so large that the disconnections athermally overcome any Peierls resistance and move at velocities approaching the speed of sound, as indicated by sonic emissions and velocity measurements. The motion is likely to be phonon damping controlled with a possible inertial contribution and the disconnections should remain nominally straight as they move, by analogy to dislocation motion at such high velocities. For slow martensite, such as that in shape memory alloys, motion by kink-pair nucleation and lateral propagation should be the operative mechanism. The disconnections should nominally remain parallel to Peierls valleys, although locally they would deviate from such parallelism because of the presence of kinks. Lateral kink propagation could occur by a thermally activated diffusional motion or by a drift mechanism involving phonon drag. The effective Peierls barrier should be greater, leading to slower disconnection velocity, in non-metallic crystals and for disconnections that are extended zonally and require shuffles as they move.

References

[1] M.S. Wechsler, D.S. Lieberman and T.A. Read, Transactions of AIME, **197,** 1503 (1953).
[2] J.S. Bowles and J.K. MacKenzie, Acta Metallurgica, **2**,129, (1954).
[3] P.G. McDougall and C.M. Wayman, “The Crystallography and Morphology of Ferrous Martensites” in *Martensite*, edited by G.B. Olson and W.S. Owen, (ASM International, USA, 1992), 59-95.
[4] R.C. Pond, S. Celotto and J.P. Hirth, Acta Materialia, **51**, 5385 (2003).

[5] R.C. Pond, J.P. Hirth, X. Ma and Y.W. Chai, "Topological Modelling of Martensitic Transformations", in *Dislocations in Solids*, edited by F.R.N. Nabarro and J.P. Hirth, (North-Holland, Amsterdam, 2007) Vol.13, 225-261.
[6] J.H. van der Merwe , Philosophical Magazine, **A45**,127 (1982).
[7] U. Dahmen, Acta Metallurgica, **30**, 63 (1982).
[8] R.C. Pond and S. Celotto, International Materials Reviews, **48**, 225, (2003).
[9] R.C. Pond, "Line Defects in Interfaces" in *Dislocations in Solids*, edited by F.R.N. Nabarro, (Amsterdam: North-Holland, 1989) Vol.8,1-66.
[10] F.C. Frank, in *Report of the symposium on the plastic deformation of crystalline solids* (Pittsburgh:Carnegie Institute of Technology, 1950), 150.
[11] B.A. Bilby, in *Report of the conference on defects in crystalline solids. London*, (Physical Society1955),124.
[12] J.P. Hirth and J. Lothe, *Theory of Dislocations*, (2nd edition Melbourne Fl:Krieger;1992).

Atomic Simulation of Twin Boundaries in HCP Metals: Mobility and Defect Interaction

Anna Serra[1] and David J. Bacon[2]

[1]Dept. Matemàtica Aplicada III, Universitat Politècnica de Catalunya (UPC), Jordi Girona 1-3, 08034 Barcelona, Spain (E-mail: a.serra@upc.edu)
[2]Department of Engineering,Brodie Tower,The University of Liverpool,Brownlow Hill, Liverpool L69 3GH, UK (E-mail: djbacon@liverpool.ac.uk)

ABSTRACT

Computer simulation is used to study the interaction of a moving $\{10\bar{1}2\}$twin boundary with straight crystal dislocations, clusters of self-interstitial atoms and vacancies, and dislocation loopsin a model of α-Zr. The interaction of crystal dislocations with twin boundaries can result in a variety of reactions, depending on the atomic structure of the boundary and the character of the dislocation. A possibly significant one is dislocation absorption by the boundary and subsequent transformation into a boundary defect that can be a source of twinning dislocations. Simulations also show that point defect clusters encountered during twin boundary motion can act as obstacles and cause strengthening by pinning twinning dislocations and restricting twin boundary motion. Furthermore, moving boundaries can act as sinks or recombination centres for defects, thereby providing a means for removing defects from regions of radiation damage.

1 Introduction

Plastic deformation in the HCP metals is partly accommodated by twinning, and therefore the mechanisms by which twins grow by motion of their boundaries and the interaction of these boundaries with other defects are of particular interest. Moreover, if the metal contains radiation damage in the form of point defects and their clusters, the interaction of twin boundaries with these defects may contribute to changes in the mechanical properties. Whereas the atomic-scale processes involved in dislocation-defect interaction have been studied extensively [1], the deformation mode associated with diffusion-less motion, i.e. not requiring mass transport, of mobile boundaries under shear stress has had little attention and is the subject of this paper. The deformation mode considered is $\{10\bar{1}2\}$twinningin a model α-Zr [2]. We study the interaction of crystal dislocations with a twin boundary and the mechanism of creation of a source of twinning dislocations and the interaction of the twin boundary with point defect clusters.

2 Simulation model

The model has about 0.5M mobile atoms and consists of two half-crystals in twin orientation separated by either a planar interface or an interface containing a twinning disconnection, i.e. a line defect with both dislocation and step character, with Burgers vector $\boldsymbol{b}_{2/2} = \frac{2}{31}[10\bar{1}1]$ (see [3,4] for details). The subscript 2/2 indicates the number of $(10\bar{1}2)$lattice planes, spacing d, at the step in the upper and lower crystals respectively. The bi-crystal has periodic boundary conditions in the glide plane x-y of the twinning dislocation and fixed boundaries (rigid blocks of atoms) in the z direction. When a twinning dislocation crosses one periodic boundary, it appears at the opposite site of the simulation box and, due to the step character, the twin interface is displaced in the z direction by the step height $2h$. The twinning dislocation is induced to glide by applying shear strain in increments of 10^{-5} via displacements of the upper rigid block. The system is relaxed to minimise the potential energy after each displacement in this static simulation (T = 0K) and the applied resolved shear stress is calculated as described in [7]. Crystal dislocations or defect clusters can be introduced on either side of the twin interface in order to consider the effect of tension below or compression above the interfacial $\boldsymbol{b}_{2/2}$ dislocation. Atoms with irregular coordination number are recorded and plotted as shown in the figures.

3 Results

3.1 Conservative movement of the $\{10\bar{1}2\}$ twin boundary.

A twin interface moves conservatively by glide of disconnections and there is a multiplicity of interfacial line defects that introduce a step and have a Burgers vector $\boldsymbol{b}_{n/n}$ parallel to the interface. The movement of such defects is, in principle, conservative although the atoms in the disconnection core shuffle to restore the correct structure. The set for which n is even includes the elementary twinning dislocation with Burgers vector $\boldsymbol{b}_{2/2}$shown in Fig.1. The small magnitude of $\boldsymbol{b}_{2/2}$ combined with the small h results in a stable defect with a wide core. Glide of this disconnection under a twinning shear stress produces conservative displacement of the boundary in the direction of its normal. Thus, a source of $\boldsymbol{b}_{2/2}$ defects that can move with the boundary provides an efficient way for twinning to proceed. We describe such a source in section 3.3.

3.2 Interaction of the twin boundary with crystal dislocations with $\boldsymbol{b} = \frac{1}{3}<11\bar{2}0>$

The interaction of a 60º crystal dislocation with the twin boundary depends on the sign of the dislocation and the relative position of the two Shockley partials with Burgers vectors $\boldsymbol{b}^{30}$ and $\boldsymbol{b}^{90}$at 30° and 90°to the dissociated line dislocation, respectively. The order of the leading and trailing partials is reversed for dislocations located on adjacent glide planes. The result of interaction of 60º dislocations of opposite line sense with the twin interface is shown on the left and right of Fig.1. The dislocation on the right (light symbol) is totally absorbed to forma $\boldsymbol{b}_{-5/-6}$boundary defect that is independent of the leading/trailing order of the dissociated crystal dislocation. The reaction on the left (dark symbol) depends on the partial order. If the $\boldsymbol{b}^{30}$partial leads, the dislocation is absorbed to create a boundary defect $\boldsymbol{b}_{3/4}$, but if the $\boldsymbol{b}^{90}$leads no absorption occurs. The resulting structure shown on the left of Fig.1is a$\boldsymbol{b}_{4/4}$ boundary dislocation that pins the $\boldsymbol{b}^{90}$partial: notice the 30º partial as two rows of atoms above the step).

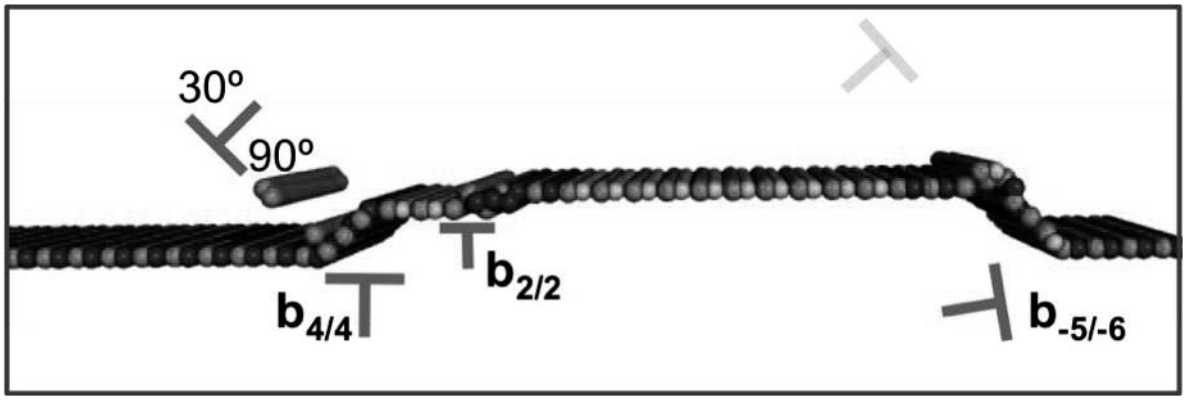

Figure 1. Twin boundary showing three boundary defects (described by the symbols below the boundary).$\boldsymbol{b}_{4/4}$ and $\boldsymbol{b}_{-5/-6}$result from interaction with crystal dislocations (shown above the boundary).

3.3 Sources of $\boldsymbol{b}_{2/2}$twinning dislocations

The small magnitude of $\boldsymbol{b}$ of this disconnection, the low Peierls stress for its glide along the interface and the easy shuffles needed to accommodate this glide favour the creation of $\boldsymbol{b}_{2/2}$dipoles in regions of the boundary where there is a stress concentration. In fact, the $\boldsymbol{b}_{2/2}$defect shown in Fig.1 has been generated in the upper part of the riser of the $\boldsymbol{b}_{-5/-6}$ defect. Under a positive (negative) shear strain the $\boldsymbol{b}_{-5/-6}$ defect acts as a source of $\boldsymbol{b}_{2/2}$ twinning dislocations that glide to the left (right) and move the boundary up (down)[5]. Importantly, the shear strain induces a conservative self-compensated climb of the $\boldsymbol{b}_{-5/-6}$ defect so that it remains in the boundary, thereby supplying the necessary twinning dislocations to maintain the conservative movement of the interface.

3.4 Interaction with point defect clusters

Clusters of self-interstitial atoms and vacancies, each containing up to 35 point defects, are introduced into one crystal. Movement of the boundary is achieved by the glide of a $\boldsymbol{b}_{2/2}$twinning dislocation of edge character under applied shear stress. Several reactions are observed, the result depending on cluster orientation and location relative to the interface plane. They include a) restriction of twin boundary mobility; b) change of cluster orientation and shape; c) glissile cluster drag by the boundary without contact; and d) total or partial absorption of a cluster by the twin boundary and cluster drag, together with simultaneous glide along the interface. It is concluded that the applied shear stress for motion of twin boundaries is raised by interaction with point defect clusters.

3.5 Interaction with dislocation loops

The interactions of the twin interface with rectangular (~9x5nm) perfect dislocation loops with $\boldsymbol{b} = \frac{1}{3}<11\bar{2}0>$ and sides lying in the basal and prism planeswere simulated.Loops were either vacancy or interstitial edge loops located in the three $\{11\bar{2}0\}$planes. Some properties of clusters are kept but, in general, the interactions with dislocation loops are more complex. As an example, Fig.2 shows a vacancy cluster with $\boldsymbol{b}$ parallel to the twinning plane. The cluster

induces loops of $\boldsymbol{b}_{2/2}$disconnections in the interface that interact with the pre-existing twinning dislocations of this boundary.

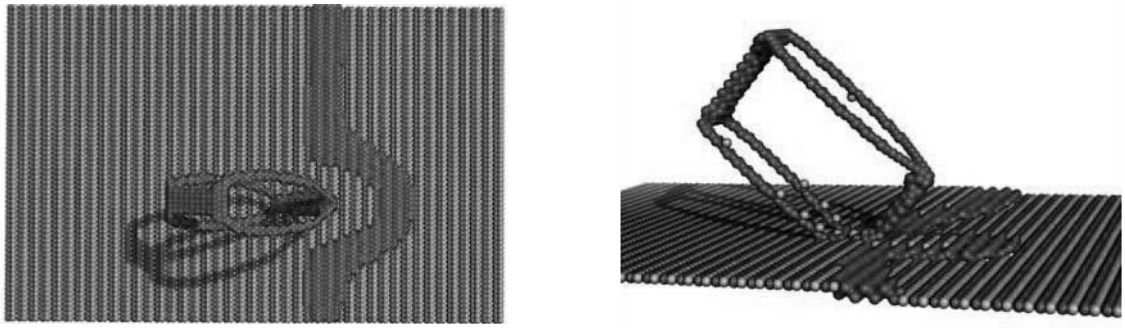

(a) (b)

Figure 2.Vacancy loop interacting with a $\boldsymbol{b}_{2/2}$ twinning dislocation that is moving from left to right in the twin boundary. Before (a) and after (b) the interface reaches the loop.

Acknowledgements

Discussions with Dr. Yu.N. Osetsky are acknowledged. A.S. was supported by the Spanish Ministry of Science and Innovation (FIS2006-12436-C02-02) and the Catalan Government (CIRIT 2005 SGR – 00779). The computing was carried out in CESCA (www.cesca.es).

References

[1] D.J. Bacon and Yu.N. Osetsky, 'Modelling dislocation–obstacle interactions in metals exposed to an irradiation environment', Materials Science & Engineering A,**400**, 353 (2005).
[2] G.J. Ackland, S.J. Wooding and D.J. Bacon, 'Defect, surface and displacement-threshold properties in α-Zr simulated with a many-body potential', Philosophical Magazine A, **71**, 553 (1995).
[3] A. Serra and D.J. Bacon, 'A model for simulating the motion of line defects in twin boundaries in the HCP metals', Zeitschrift für Metallkunde, **95**, 4 (2004).
[4] A. Serra and D.J. Bacon, 'Modelling the motion of $\{11\bar{2}2\}$twinning dislocations in the HCP metals', Materials Science and Engineering A,**400**, 496 (2005).
[5] A. Serra and D.J. Bacon, 'A new model for $\{10\bar{1}2\}$ twin growth in h.c.p. metals', Philosophical Magazine A,**73**, 333 (1996).
[6] A. Serra, D.J. Bacon and Yu.N. Osetsky, 'Strengthening and microstructure modification associated with moving twin boundaries in hcp metals', Philosophical Magazine Letters ,**87**,451 (2007).
[7] Yu.N.Osetsky and D.J. Bacon, 'An atomic-level model for studying the dynamics of edge dislocations in metals', Modelling Simulation Materials Science Eng., **11**, 427 (2003).

Dislocation activity within nanocrystalline metals: A molecular dynamics study

Christian Brandl, Erik Bitzek, Peter M. Derlet, Helena Van Swygenhoven

Materials Science & Simulation, ASQ/NUM, Paul Scherrer Institut, CH-5232 Villigen PSI, Switzerland (E-mail: christian.brandl@psi.ch)

ABSTRACT

The use of large scale molecular dynamics to study the mechanical properties of FCC nanocrystalline (nc) metals provides a detailed picture of the atomic-scale processes during plastic deformation at room temperature. Simulations have revealed interface dominated processes such as grain boundary sliding and migration, and intragranular deformation processes involving dislocation activity. In particular grain boundaries can act as both sources and sinks for partial or full dislocations and the surrounding grain boundary environment can significantly affect the motion of a dislocation as it propagates through the grain. Simulations have now revealed that cross-slip also occurs in nc-Al simulations, and that the grain boundary structure is found to strongly influence when and where cross-slip occurs, allowing the dislocation to avoid local stress concentrations that otherwise can act as strong pinning sites for dislocation propagation. More generally, statistical properties of dislocation activity in the nanocrystalline Al simulations are discussed in the context of micromechanical models on nanocrystalline plasticity.

1. Introduction

The search for understanding of the deformation mechanism in nanocrystalline (nc) metals has widely profited from the use of molecular dynamics (MD) simulation, revealing grain boundary (GB) accommodation processes such as GB sliding and intragranular slip involving dislocation nucleation and absorption at GBs [1]. Additional to the simple picture of planar dislocation propagation through the grain, the GB structure can force a screw dislocation to leave its initial habit plane via cross slip in order to find the most effective dislocation pathway through the grain [2]. Dislocation interaction with GBs, nucleation and propagation, depends on the local character of the GBs. Therefore the stresses related to the dislocation-GB interaction will be characterized by a distribution, which can be linked to meso-scale models. In the present work the effect of cross-slip on the stress-strain curve is discussed in terms of strain hardening.

2. Computational Procedure

A standard large scale molecular dynamics simulation was performed at a constant temperature of 300 K and a constant strain rate of 1e8 /sec. Periodic boundary conditions were imposed in all

three dimensions. The uniaxial strain was modeled by longitudinal continuous constant scaling of the box-size and by using a zero stress condition in the transversal directions utilizing the Parrinello-Rahman barostat [3]. The nc microstructure for the 100 grain sample with a mean grain size of 11.5 nm was constructed via the Voronoi tessellation procedure as described in detail in ref. [4]. The interatomic forces and energies were modeled by the embedded atom model potential for Al [5], which is known to result in the nucleation of perfect dislocations within the MD time scale, since the ratio of unstable to stable stacking fault energy is close to unity [6]. For analysis at the atomic level, the medium range order (MRO) procedure is used in which atoms colored according to their local crystallographic class: gray represents face centered cubic (FCC) atoms, red hexagonal closed packed (HCP) atoms, green other 12-coordinated atoms and blue non-12-coordinated atoms.
The local atomic stress tensor was determined by the atomic virial atomic formulation [7]. The grain average resolved shear stresses (GRSS) was calculated from the local stress tensor of all FCC atoms in a grain and decomposed into the 12 slip system shear components of the FCC crystal.

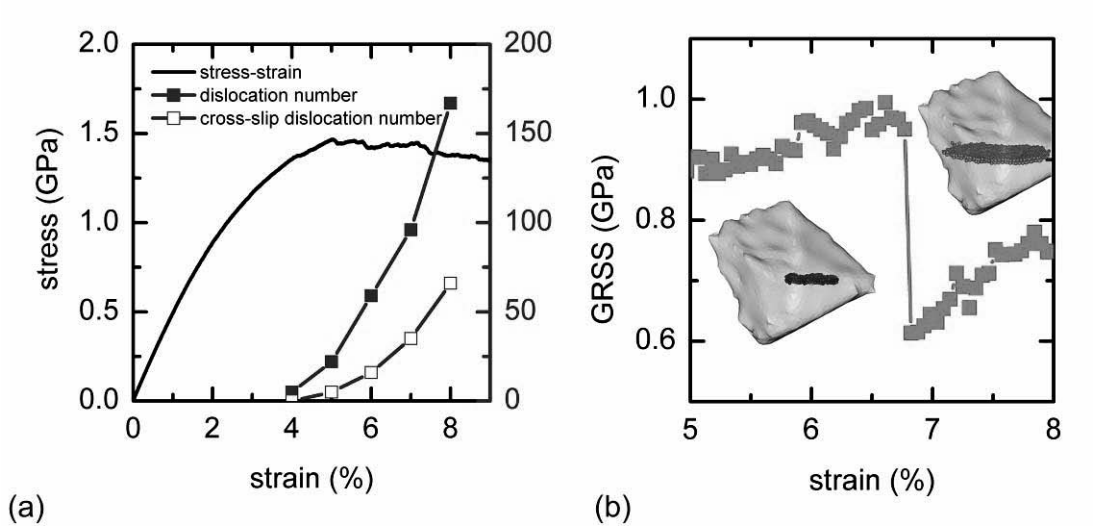

Figure 1. (a) (Left axis) Stress-strain for a constant strain rate of 1e8 /sec. (Right axis) Total cumulative number of dislocation (filled blue squares) and number of these dislocations that have cross-slipped as a function of strain (opened blue squares). (b) Grain averaged resolved shear stress (GRSS) of one particular grain. The insets display the slip before (lower left) and after (upper right) the discrete stress drop. The atoms are coloured according to the Burgers vector length (partial Burgers vector blue; perfect Burgers vector green). The gray volumetric regions visualize the grain shape.

2. Stress-Strain Curve and Dislocation Activity

Fig. 1a (left axis) displays the resulting stress-strain curve, and an extended elastic-plastic transition regime is seen until a flow stress of approximately 1.5 GPa. Beyond this region the flow stress decreases with increasing total strain. From inspection of the slip traces the dislocation activity was enumerated and is presented in Fig. 1a (right axis). Significant dislocation propagation begins at ~4 %; just before the maximum flow stress is reached. A delay

in the onset of macroscopic plasticity was also observed experimentally [8]. Before the onset of dislocation based plasticity, the elastic-plastic transition regime is predominately controlled by grain boundary processes, such as GB sliding, atomic shuffling and GB migration; and by nucleation of the leading or even the trailing partial dislocations that do not propagate [9]. Furthermore Fig. 1a shows the number of these dislocations that cross-slip, and reveals that the likelihood for cross slip occurring increases with strain.

Using GRSS the stress history was analyzed at the grain level. Fig. 1b shows a typical example of the GRSS as a function of strain. The insets display the slip before and after the stress drop at 6.8 %. Evidently, dislocation propagation causes a stress relaxation at the grain level. Hence the stress state before the drop can be taken as a measurement of slip resistance. The distribution of critical GRSS throughout the simulation up to a total strain of 8.5 % is shown in Fig. 2.

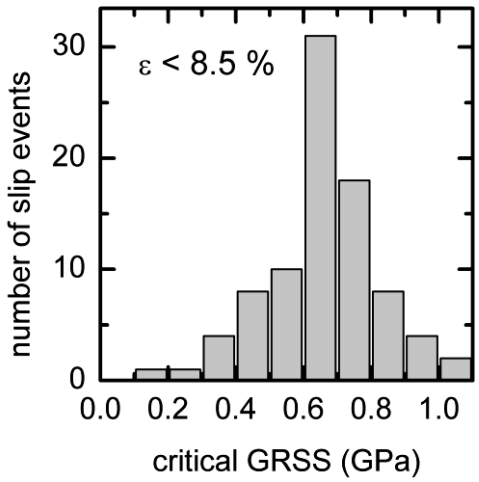

Figure 2. Histogram of critical GRSSs [9] (as for example shown in Fig. 1b).

The distribution is characterised by a mean value of ~700 MPa. Detailed analysis of the mechanism reveals a correlation with the critical GRSS in the following manner [9]:

- Dislocations at a high GRSS (~900 MPa) nucleate and subsequently propagate unhindered through the grains.
- Dislocation processes at an intermediate GRSS (500 – 900 MPa) exhibit a temporal separation between nucleation and propagation due to the pinning-depinning mechanism [1]. In other words dislocation propagation is a distinct mechanism from the dislocation nucleation. Furthermore, in this GRSS regime (double-) cross-slip usually occurs.
- Dislocation processes at a low GRSS (smaller 500 MPa) exhibit more complex processes which can include a change of the involved grain boundary structure, dislocation-dislocation interaction, or dislocation cross-slip. For example, GB dislocations in small angle GBs propagate through the grains causing grain coalescence.

The majority of the dislocation events operate in the intermediate GRSS regime and therefore the presented simulation supports the picture that dislocation mediated plasticity in nanocrystalline FCC metals is predominantly controlled by dislocation propagation in high the strain rate regime of MD.

3. Dislocation Cross-Slip

As already mentioned, the GRSS statistics points towards the importance of the dislocation propagation which is hindered by the local GB structure (e.g. ledges and misfit structures) [1] and cross-slip is observed [2]. In this section the importance of the GB structure becomes even clearer since dislocations can bypass these pinning sites via cross slipping screw segments.

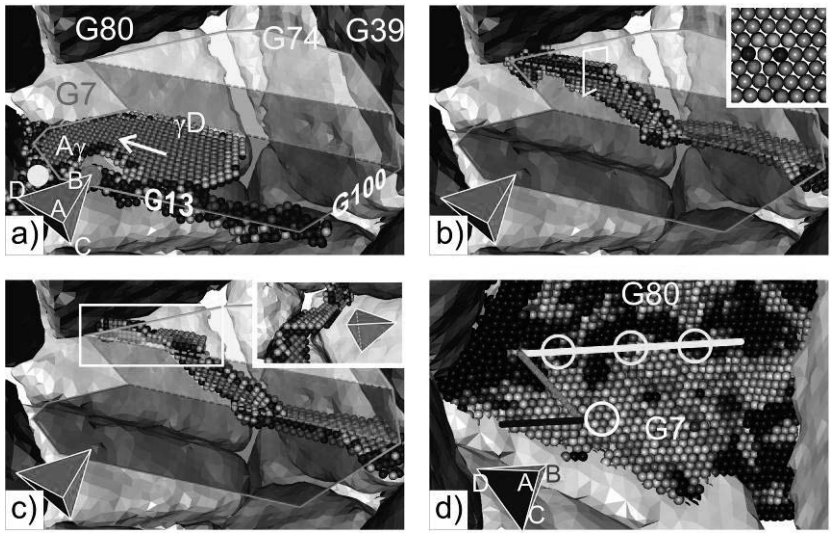

Figure 3. (a)-(c) Three snapshots of a perfect dislocation that cross-slips twice to avoid potential pinning sites of the GB 86-7 shown by the compressive stress regions in (d) [2]. Only non-FCC atoms within the grain are shown. The pressure in (d) ranges from -1.5 GPa tensile (blue) to 1.5 GPa (red) compressive stress (adapted from [2]).

Fig. 3 a-c display the temporal sequence of such a dislocation as it cross-slips through grain 86. The gray volumes visualize some of the neighbouring grains. Only the dislocation cores (blue and green atoms) and the stacking fault (red atoms) are shown according to there medium range order. The leading partial dislocation nucleates at the triple junction [indicated by the yellow dot in Fig. 2a] whereas the trailing partial dislocation nucleates at the GB 86-13 [indicated by the light blue dot in Fig. 2a] resulting in a perfect dislocation with the Burgers vector AD according the Thompson tetrahedron shown in Fig. 3a-d. This dislocation propagates on the (c)-plane [indicated by the transparent blue area in Fig. 3] until the left dislocation end encounters a highly compressed GB region (GB 86-7) [indicated by the white circle in Fig. 3d]. Here the dislocation cross-slips onto the plane (b) [indicated by the transparent magenta area in Fig. 3]. During subsequent propagation (Fig. 3 b and 3 c), the edge segment moves to the right whilst the screw segment double cross-slips back onto another (c)-plane [indicated by transparent yellow area in Fig. 3a-c] resulting in an evolving stair rod structure [see for example upper right inset in Fig. 2b]. Before the dislocation is absorbed into the GB on the new habit plane (c), the dislocation is seen to make three attempts to cross slip onto other (b)-planes [see upper right inset in Fig. 3c and locations indicated by yellow circles in Fig. 3d]. Close inspection of the 1st cross slip region reveals that the compressive stress states in the GB 7-86 is caused by a misfit structure, which accommodates the misorientation between the grains. Therefore cross-slip allows a dislocation to avoid compressive regions in a GB where the edge component otherwise has to be deposited and

hence the dislocation is able to be deposited in more favoured tensile region such as a triple line (indicated by yellow line in Fig. 3d).
The occurrence of cross-slip, which is classically known to reduce the strain hardening in stage 3 of single crystal plasticity, also explains why in nanocrystalline metal no strain hardening in the simulation is observed beyond yielding. Former MD simulations showed relief of stress intensities upon dislocation nucleation [1] [10] [11], but at the same time new stress intensities are built up due to the lack of GB relaxation upon arrival of new dislocations within the MD time frame [12] [13]. Such an accumulation does not lead to an increase of the flow stress with increasing strain (Fig. 1a) and can be understood when dislocations are able to circumvent these new stress intensities via cross-slip.

4. Conclusion/Summary

Projecting the details of MD towards meso-scale models, the following issues should be taken into account [9]:

- A distribution of the slip plane areas for a given grain size.
- A distribution of the critical resolved shear stresses required to trigger slip events.
- The incorporation of a distribution of dislocation sources that are activated at shear stresses lower than that required for the dislocations to propagate.

Furthermore the additional degree of freedom in dislocation pathways – namely via cross-slip – brings an important new aspect to the subject of dislocation propagation within nc environment, since this mechanism enables dislocation to bypass pinning sites.

Acknowledgements

The authors acknowledge the financial support of European Commission (FP6-NANOMESO, Grant No. 016710) and thank the Swiss National Supercomputing Centre for the use of their computing facilities.

References

[1] H. Van Swygenhoven, P. M. Derlet, and A. G. Froseth, "Nucleation and Propagation of Dislocations in Nanocrystalline Fcc Metals", Acta Materialia, **54**, 1975 (2006).
[2] E. Bitzek, C. Brandl, P. M. Derlet, and H. Van Swygenhoven, "Dislocation Cross-Slip in Nanocrystalline Fcc Metals", Physical Review Letters, **100**, 235501 (2008).
[3] M. Parrinello and A. Rahman, "Polymorphic Transitions in Single Crystals: A New Molecular Dynamics Method", Journal of Applied Physics, **52**, (1981).
[4] P. M. Derlet and H. Van Swygenhoven, "Atomic Positional Disorder in Fcc Metal Nanocrystalline Grain Boundaries", Physical Review B, **67**, 014202 (2003).
[5] Y. Mishin, D. Farkas, M.J. Mehl, and D.A. Papaconstantopoulos, "Interatomic Potential for Al and Ni from Experimental Data and Ab Initio Calculations", Materials Research Society Symposium Proceedings, **538**, 535 (1999).

[6] H. Van Swygenhoven, P. M. Derlet, and A. G. Froseth, "Stacking Fault Energies and Slip in Nanocrystalline Metals", Nature Materials, **3**, 399 (2004).
[7] D. H. Tsai, "The Virial Theorem and Stress Calculation in Molecular Dynamics", The Journal of Chemical Physics, **70**, 1375 (1979).
[8] S. Brandstetter, H. Van Swygenhoven, S. Van Petegem, B. Schmitt, R. Maass, and P. M. Derlet, "From Micro- to Macroplasticity", Advanced Materials, **18**, 1545 (2006).
[9] E. Bitzek, P. M. Derlet, P. M. Anderson, and H. Van Swygenhoven, "The Stress-Strain Response of Nanocrystalline Metals: A Statistical Analysis of Atomistic Simulations", Acta Materialia, **In Press**, (2008).
[10] H. Van Swygenhoven, P. M. Derlet, and A. Hasnaoui, "Atomic Mechanism for Dislocation Emission from Nanosized Grain Boundaries", Physical Review B, **66**, 024101 (2002).
[11] P. M. Derlet, H. Van Swygenhoven, and A. Hasnaoui, "Atomistic Simulation of Dislocation Emission in Nanosized Grain Boundaries", Philosophical Magazine, **83**, 3569 (2003).
[12] P. M. Derlet, S. Van Petegem, and H. Van Swygenhoven, "Calculation of X-Ray Spectra for Nanocrystalline Materials", Physical Review B, **71**, 024114 (2005).
[13] S. Brandstetter, P. M. Derlet, S. Van Petegem, and H. Van Swygenhoven, "Williamson-Hall Anisotropy in Nanocrystalline Metals: X-Ray Diffraction Experiments and Atomistic Simulations", Acta Materialia, **56**, 165 (2008).

Dynamic Observations of Heavy-ion Damage in Fe and Fe-Cr Alloys

M. L. Jenkins[1], Z. Yao[1], S. Xu[1], M. Hernandez-Mayoral[2] and M. A. Kirk[3]

[1] Department of Materials, University of Oxford, Parks Rd., OX1 3PH
mike.jenkins@materials.ox.ac.uk, zhongwen.yao@materials.ox.ac.uk, sen.xu@materials.ox.ac.uk
[2] Division of Materials. Avenida Complutense, CIEMAT, 22, 28040-Madrid Spain, m.mayoral@ciemat.es
[3] Material Science Division, Argonne National Laboratory, Argonne, IL60439, kirk@anl.gov

ABSTRACT

Thin foils of pure Fe and Fe 5-11%Cr alloys were irradiated with 100-150 keV Fe^+ and Xe^+ ions at 20°C, 300°C and 500°C in the IVEM-Tandem Facility at Argonne National Laboratory. Dynamic TEM observations followed the evolution of damage over doses ≤ 13dpa. Several new observations of interest to modelers were made:

- Small 2-4nm dislocation loops with <100> and ½ <111> Burgers vectors first appeared at doses 0.01-0.1 dpa , much higher than in many other materials.
- The contrast of new loops developed over time intervals as long as 0.2s, many orders of magnitude longer than expected for a process of cascade collapse.
- Loop hopping and loss of loops to the surface was induced by both ion irradiation and the sub-threshold electron beam alone.
- In Fe the number of loops retained was strongly dependent on the foil orientation; less loop loss occurred in FeCr alloys.
- At doses greater than about 1 dpa, complex microstructures developed in thicker regions of foils, but these microstructures were quite different at 500°C than at lower irradiation temperatures. In Fe irradiated at 300°C the damage took the form of interstitial loops with **b** = ½<111>. Large finger-shaped loops developed by the growth and coalescence of smaller loops. At 500°C in the same material large loops with **b** = <100> developed.
- Similar damage structures developed in Fe8%Cr, although on a finer scale than in pure Fe. At 20°C and 300°C most loops had b = ½<111>; at 500°C most were <100>.

Several of these observations are consistent with recent modeling, as will be discussed.

The IVEM-Tandem Facility at ANL is supported by the US DOE Office of Science. Part of this work was funded by the UKAEA, Culham Science Centre.

Molecular Ion Irradiations of Molybdenum

C A English[1,2] and M L Jenkins[2]

[1] Nexia Solutions, Harwell Business Centre, Didcot, Oxon OX11 0RA
(E-mail: colin.a.english@nexiasolutions.com)
[2] Department of Materials, University of Oxford, Parks Road, Oxford OX1 3PH,
(E-mail: mike.jenkins@materials.ox.ac.uk)

ABSTRACT

We have carried out a series of TEM experiments to investigate systematically the role of the cascade energy density and vacancy concentration in the collapse of displacement cascades to vacancy dislocation loops in molybdenum. Single-crystal [011] and [001] foils of high-purity molybdenum were irradiated with Sb^+ single ions and Sb_2^+ and Sb_3^+ molecular ions. Three different ion energies were employed (60keV, l20keV and 180keV) in order to vary systematically the total cascade energy (the energy per ion) and the energy per atom. Loop sizes and defect yields were found to be larger for molecular ions than for single ions at constant cascade energy. The defect yield was typically three times larger for Sb_3^+ molecular ions than for single ions of the same energy. In [011] foils most loops had Burgers vectors **b** = ½<111> lying in the plane of the foil. However in molecular ion irradiations a small fraction of loops with **b** = <100> was also found. This fraction was higher for Sb_3^+ than for Sb_2^+ ions and also increased with ion energy. In [001] foils defect yields were much smaller because of the loss of glissile ½<111> loops to the surface, but < 100> loops were still present in molecular ion irradiations. In Sb_3^+ irradiations of [001] foils a large majority of loops had **b** = <100>. These results will be compared with recent molecular dynamics simulations of the effect of the mass of primary knock-on atoms on displacement cascades debris in iron by D.J. Bacon's group [1]

[1] A.F Calder., D.J., Bacon A.V. Barashev and Yu.N Osetsky, "Effect of Mass of the Primary Knock-on Atom on Displacement Cascade Debris in α-iron", Philosophical Magazine Letters **88** 43 (2008).

Atomic-scale Modeling of Helium Atoms and Vacancies in Dislocations in alpha-Iron

Howard Heinisch

Pacific Northwest National Laboratory, MS P8-15, P.O. Box 999, Richland, WA,USA
(E-mail: hl.heinisch@pnl.gov)

ABSTRACT

Atomic-scale Modeling of Helium Atoms and Vacancies in Dislocations in alpha- Iron H.L. Heinisch, F. Gao and R.J. Kurtz Pacific Northwest National Laboratory, Richland WA, USA Helium is known to cause embrittlement of steels and other metals, and its presence is inescapable in the structural materials of a fusion reactor, including the low activation ferritic steels that are candidates for near-term fusion devices. Experimental evidence indicates that helium accumulates on dislocations, at grain boundaries, and particle-matrix interfaces in ferritic steels, leading to bubble formation and embrittlement of the material. The possibility that knowledge-based alloy design can provide steels that are resistant to the effects of helium requires at the very least an understanding of the kinetics and dynamics of helium atoms in and near these microstructures. Multiscale modeling, from first principles atomistic simulations to mesoscale descriptions of embrittlement and cracking, is being developed to address this problem. We report here on results of modeling He-dislocation interactions using molecular statics, molecular dynamics and transition state energy determinations of helium atoms, vacancies and helium-vacancy clusters near and within dislocations in alpha-iron. It is found that both vacancies and helium atoms are trapped in the core of a screw dislocation, and they migrate along these dislocations with similar migration energies, thus enhancing the nucleation and growth of He bubbles. The sensitivity of these results to the choice of interatomic potentials will also be discussed.

Atomic-Level Modeling of Migration of Vacancies, He Interstitials, and Nucleation of He-V clusters at Grain Boundaries in alpha-Fe

Fei Gao

Pacific Northwest National Laboratory, 902 Battelle Boulevard, P. O.Box 999, Richland, WA, USA (E-mail: fei.gao@pnl.gov)

ABSTRACT

Atomic-Level Modeling of Migration of Vacancies, He Interstitials, and Nucleation of He-V clusters at Grain Boundaries in alpha-Fe F. Gao, H.L. Heinisch and R.J. Kurtz Pacific Northwest National Laboratory, Richland, WA 99352, USA One of the most important issues for fusion materials development is the high rate of production of helium, and its interaction with microstructural features. Helium trapping and interactions with dislocations, grain boundaries (GBs) and particle-matrix interfaces can result in adverse effects on mechanical properties of metals and alloys. In particular, high helium concentrations can lead to the formation of helium bubbles that enhance void swelling and cause embrittlement by intergranular fracture along GBs. Thus, the formation of He bubbles both in the bulk and at GBs remains one of the most important aspects in nuclear fusion technology. In order to explore the microstructural evolution of materials in a fusion reactor environment, it is necessary to fundamentally understand the behavior of lattice defects and helium atoms in the materials, particularly with respect to their interactions with various sinks. The dimer method for searching transition states has been used to systematically search for possible migration paths of vacancies, He interstitials and He-vacancy (He/V) clusters at the sigma 11<110> {323} and the sigma 3<110> {111} GBs in alpha-Fe. Individual vacancies can migrate to and become trapped at the GBs. These trapped vacancies can diffuse along the GBs with migration energies less than that within a perfect crystal, and in one-dimensional fashion along specific directions in both GBs. Also, dimer saddle point searches show that He interstitials can diffuse along the GBs with migration energies of 0.4-0.5 eV, similar to those of individual vacancies at the GBs. However, it is of interest to note that He atoms migrate two-dimensionally in the sigma 3 boundary, and one-dimensionally in the sigma 11 boundary. We have further developed the dimer method to deal with flexible boundary conditions, which is important for studying the properties of large He-V clusters at GBs. Long-time dynamics based on the dimer method has been employed to investigate the possible nucleation mechanisms of He-V clusters as a function of the number of He interstitials and vacancies in bulk and GBs. The sensitivity of these results to different interatomic potentials will also be discussed.

Corresponding Author: F. Gao fei.gao@pnl.gov Pacific Northwest National Laboraroty P.O. Box 999 K8-93 Richland WA 99352

Resistance to Fast Dislocation Motion

Chung H. Woo

The Hong Kong Polytechnic University, Hung Hom, Kowloon, Hong Kong, SAR Nil
(E-mail: chung.woo@polyu.edu.hk)

ABSTRACT

Conceptually, the dynamics of a dislocation can be simply considered in terms of motion driven by a generalized force and opposed by resistances due to dissipative reactions with various components of the real solid. These include the discrete structure and symmetry of the crystal lattice, scattering due to real and virtual particles, such as electrons, phonons and magnons, and other crystal defects. Early calculations based on continuum linear elastodynamics, taking into account various dissipative mechanisms, found that at a sufficiently high speed (> 0.1 cs), the dislocation follows a viscous motion under a drag force proportional to the velocity. Acceleration of the dislocation beyond sound speed cs is not permissible due to the progressively increasing radiation drag as the dislocation approaches cs. Due to the dominance of the phonon and magnon effects as temperature increases, the viscous drag on the dislocation generally increases with increasing temperature, except at very low temperatures or very low driving forces. In such cases, effects of defect barriers and electron scattering are the dominant factors. The predictions of these calculations are generally in good agreement with experiments for dislocation velocities much below the sound speed. However, the situation is much less clear for higher dislocation velocities, both experimentally or theoretically. Linear elastodynamics is evidently inadequate for the description of dislocation motions in a discrete crystal lattice. Effects due to configurational oscillation as the dislocation core sequentially attains the ground-state and saddle-point configurations, or effects on the dispersion relations due to the discreteness of the lattice, lie beyond its scope. Thus, molecular dynamics (MD) simulations observed motion of dislocations crossing the subsonic/transonic boundary, which is forbidden in linear elastodynamics. To obtain information on the resistance to dislocation motion due to lattice discreteness, we have conducted systematic investigations on the dynamics of fast dislocations as a function of temperature and applied shear in a bcc Mo and W using molecular dynamics simulation. The results reveal very large fraction of the energy input is dissipated as heat generated from the dislocation core, producing dislocation drag that is an order of magnitude larger than those based on the continuum theory.

Hardening by completely and partially absorbed ½<111> and <100> dislocation loops reacting with dislocations in α-Fe.

D. Terentyev[1], D.J. Bacon[2], P. Grammatikopoulos[2] and Yu.N. Osetsky[3].

[1]SCK-CEN, Nuclear Material Science Institute, Boeretang 200, B-2400, Mol, Belgium
[2]Materials Science and Engineering, Department of Engineering, The University of Liverpool, Brownlow Hill, Liverpool L69 3GH.
[3]Computer Sciences and Mathematics, ORNL, Oak Ridge, TN 37831, USA

ABSTRACT

Molecular dynamics simulations were used to investigate reactions between an ½<111>{110} edge dislocation with interstitial dislocation loops with Burgers vector equal to either ½⟨111⟩ or ⟨100⟩. The loop size was varied from 0.5 nm up to 8.6 nm, and simulations of both static and dynamic conditions were performed. The results obtained show that small loops (with size up to ~1nm) are easily absorbed by reaction with edge dislocations, independently of their Burgers vector. Large loops are strong obstacles and, depending on the difference in orientation of the dislocation and loop Burgers vectors, are either completely or partially absorbed. The mechanism that provides complete absorption of relatively large loops involves propagation of the reaction segment, formed in favourable dislocation reaction, over the loop surface. This motion is controlled by cross-slip of the screw dislocations formed in a dipole and can involve complicated dislocation reactions. Thus, thermally-activated glide and/or decomposition of the pinning segment formed in the favourable reaction determines both the absorption and critical stress, and therefore depends on temperature, strain rate and loop size.

1. Introduction

The microstructure of neutron-irradiated ferritic alloys, which are important structural materials for nuclear reactors, typically consists of dislocation loops, nano-voids and second-phase particles. At sufficiently high doses (a few dpa), defects detectable by transmission electron microscopy (TEM) in bcc Fe and Fe-based alloys are mainly self-interstitial atom (SIA) dislocation loops (henceforth DLs) with Burgers vector, $\boldsymbol{b}_L$, equal to either ½<111> or <100> (see [1,2] and references cited therein). DLs present in the matrix pin dislocations by either contact or elastic interaction and obstruct their motion, which leads to an increase of the yield stress and reduction in ductility. Furthermore, experiments suggest that the ability of dislocations to absorb DLs assists in the formation of defect-free channels, which may cause plastic instability and loss of work hardening [3]. Rationalization of these phenomena requires detailed understanding of the interaction mechanisms between dislocations and radiation-induced defects, including dislocation loops. This can be provided by atomic-scale computer simulations using molecular dynamics (MD) techniques. In such simulations, shear strain, γ, is applied at a

constant rate, $\dot{\gamma}$, to a model crystal containing a dislocation line and loop, and the corresponding shear stress, τ, is calculated from the reaction force exerted on the sheared boundaries by the crystal [4].

A series of MD studies has been focused on the interaction of a ½<111>{110} edge dislocation with a periodic row of DLs in iron with $\boldsymbol{b}_L$ equal to either ½<111> or <100> [5-9]. For the ½<111> loops it has been revealed that those with $\boldsymbol{b}_L$ parallel to the dislocation glide plane (DGP) do not offer significant resistance to the glide of an edge dislocation and can be easily absorbed or dragged by it: we do not consider them further here. DLs with $\boldsymbol{b}_L$ inclined to the DGP are attracted by an edge dislocation and react with it [7]. Small DLs (e.g. containing up to 37 SIAs) are easily absorbed as superjogs on the dislocation line [7]. Larger ones (>100 SIAs) react with the dislocation to form a segment with $\boldsymbol{b}$ of <100> type, which is sessile in the DGP and thus pins the dislocation [5,7,8]. The reaction mechanism and the critical stress, τ_C, required to unpin the dislocation was found to depend on temperature and loop size [5-8]. The results obtained so far suggest that even relatively large ½<111> loops (331 SIAs) can be completely absorbed at sufficiently high temperature (≥300K). Favourable reactions with <100> loops form ½<111> segments and, in contrast with ½<111> DLs, have a wider variety of outcomes, ranging from no to total loop absorption by the edge dislocation [9]. Furthermore, <100> DLs with $\boldsymbol{b}_L$ laying in the dislocation slip plane are strong barriers to dislocation glide, others are weak.

The main goal of the present work is to review details of absorption of <100> and ½<111> loops by reaction with an edge dislocation and the factors controlling it. We therefore used MD simulations to study reactions of the edge dislocation with DLs with size varied from 0.5nm (invisible in a TEM) up to 8.6nm (easily resolvable), in both static (T = 0K) and dynamic (T = 1 - 600K) conditions.Headings (e.g. Introduction, Procedure, Numerical Methods, Results, Discussion, etc.) should be in 12 pt, bold and title case. Please number headings (1., 2., 3., etc). Provide one space between heading and text and double spaces between text and following heading.

2. Simulation technique

The ½[111]($1\bar{1}0$) edge dislocation was constructed using the model of a periodic array of dislocations developed in [4]. Dislocation glide occurred by applying a [111]($1\bar{1}0$) shear strain at a constant rate, $\dot{\gamma}$, in the range from 10^6 to 5×10^7 s^{-1}. The corresponding stress-strain relationships ($\tau-\gamma$) for the dislocations reacting with loops were obtained, by estimating the stress acting on the fixed parts of the MD crystallite subject to displacement [4].

A straight edge dislocation was formed in the MD cell and the atoms relaxed to minimize potential energy before the DL was created, after which relaxation was performed again. The model was then equilibrated at the chosen temperature, T, prior to application of shear strain. Circular ½<111> SIA loops were placed below the dislocation slip plane, while square <100> loops (with sides oriented along <110> directions) were placed so that the dislocation could intersect them. The number of defects in the DLs was varied from 37 up to 1225 interstitials. Simulation of reactions with the largest loops was performed in crystals containing up to 6M of atoms, whereas reactions involving smaller loops were modelled in crystals containing ~1M of atoms. The length of the dislocation line (L) was varied from 20.5nm up to 61.5nm and the crystal size along [111] direction was varied from 100b up to 200b depending on the DL size and

simulation temperature, to avoid the self interaction of the dislocation via periodic boundary (along [111] direction). The size of the crystal along $[1\bar{1}0]$ direction was kept constant equal to 20nm. Thus, the dislocation density was varied in the range $1\text{-}2\times10^{15}$ m^{-2}, resulting in the equilibrium dislocation velocity (in the range of above-specified strain rates) ranging from 2 to 200 m/s.

All simulations were performed within NVE ensemble without additional temperature control. MD integration time step was 5fs for simulations at 1K and 2fs at higher T. All simulations used the many-body interatomic potential for Fe from [10]. Identification of the dislocation line and dislocation loops was realized via atomic disregistry and/or coordination number and/or potential energy deviation analyses [4]. For understanding of the dislocation reactions introduced later, the direction of the Burgers vector and line sense is as defined by the RH/FS convention, e.g. [11].

3. Results and discussion

3.1. Absorption of ½<111> loops

Two reaction mechanisms resulting in compete absorption by the edge dislocation of DLs (with $\boldsymbol{b}_L$ equal to either $\frac{1}{2}[1\bar{1}1]$) or $\frac{1}{2}[\bar{1}11]$ inclined to the $(1\bar{1}0)$ glide plane) have been reported [5,7,8]. In one ($\boldsymbol{b}_L=\frac{1}{2}[1\bar{1}1]$ [7,9]), the reaction forms a <100> segment which pins the dislocation and causes a screw dipole to form on the dislocation as it bows forward under increasing τ. Eventually, the reaction segment glides across the loop surface and converts $\boldsymbol{b}_L$ to $\frac{1}{2}[111]$. In the other ($\boldsymbol{b}_L=\frac{1}{2}[\bar{1}11]$) [5,9]), the <100> reaction segment splits into two screw segments, which also glide across the loop surface and convert it into a set of superjogs. Here, we have observed both mechanisms, but complete or even partial loop absorption did not occur in all reactions. As demonstrated already in [7], small ½<111> loops (up to 37 SIAs) change $\boldsymbol{b}_L$ spontaneously to that of the dislocation and the absorption process does not require an additional stress. With the interatomic potential used here, the smallest loop to undergo spontaneous absorption at 300K contained 37 SIAs (diameter D~1.5 nm), while additional stress was required for a loop containing 61 SIAs (D~1.9 nm). Furthermore, the stress needed for the absorption reaction to proceed increases approximately linearly with D for simulations at the same T and $\dot{\gamma}$, as seen in Fig. 1(a) for 300K and $10^7 s^{-1}$. Thus, the absorption of relatively large SIA loops (1.5-4.5 nm) occurs at high stress. The largest loop (D=8.6nm containing 1225 SIAs) was not absorbed in the same simulation conditions, however, for the two screw arms forming the pinned dipole were seen to glide towards each other in the DGP and annihilate at τ_C.

Loop size is not the only factor controlling absorption. As noted above, absorption of relatively large DLs requires motion of the <100> reaction segment across the loop surface, and this occurs under the action of cross-slip of the two screw side arms of the dislocation as it bows out [7,8]. The stress (say $\tau_{<100>}$) required for glide of the <100> segment and/or cross-slip of a screw dipole appears to depend on T, since a significant decrease of τ_C in reactions with $\frac{1}{2}[1\bar{1}1]$ loops was observed in [8] for simulations above 300K and was found here as well (see Fig. 1(b)). In low-T simulations, when $\tau_{<100>}$ is relatively high and the reaction segment less mobile, the screw dipole simply extends under the applied stress. On reaching sufficient length, the screw arms glide (in the DGP) under their mutual attraction, annihilate and release the dislocation from the loop.

Thus, the probability of absorption decreases with decreasing T at fixed D and $\dot{\gamma}$. Furthermore, it is observed that the probability decreases with increasing $\dot{\gamma}$. This is due to a combination of the low mobility of the <100> reaction segment and rapid elongation of the screw dipole, which allows the two screw dislocations to reach a length when they annihilate by glide in the DGP rather than cross-slip.

Below we present a few illustrative examples. Reactions with a ½[1$\bar{1}$1] loop of 169 SIAs (D=3.2nm) at $\dot{\gamma}=10^7 s^{-1}$ result in complete absorption for T > 100K. In low-T or simulations, the dipole annihilates via glide of the screw dislocations, with the result that no absorption occurs. The configuration of the dislocation and loop at τ_C for T=0K (static simulations) is shown in Fig. 2(a). Note the large difference in τ_C for the reactions at 0 and 300K in the plot of Fig.1(b). For large loops, $\tau_{<100>}$ is sufficiently high for the screw dipole to grow and reach the critical length for annihilation even at relatively high temperature (e.g. 300K). The situation where glide of the <100> reaction segment and closure of the screw dipole by glide of screw arms are competing processes occurs for a 4.6nm ½[1$\bar{1}$1] DL (containing 360 SIAs) at 300K. The dislocation configurations at τ_C and the stress-strain curves obtained at different $\dot{\gamma}$ are presented in Fig.3. It is clear that the dipole is much shorter at τ_C for lower strain rate (Fig.3(a)), where complete absorption occurs. Reactions at higher $\dot{\gamma}$ lead to partial absorption only. Again, there is a significant difference in τ_C for low and high $\dot{\gamma}$.

3.2. Absorption of [001] loops by the edge dislocation

Let us first describe the observed absorption mechanism and then discuss factors controlling it. Visualization snapshots extracted from MD simulations showing the dislocation-DL configurations with increasing time for reactions involving [001] loops containing 169 SIAs are presented in Fig. 4. The square loops have [110] and [1$\bar{1}$0] sides. The uppermost loop segment has direction [110] and lies in the dislocation slip plane in Fig.4(a1) and the centre of the loop is located in the dislocation slip plane in Fig.4(b1). The interaction process in these reactions is as follows.

a) The dislocation is initially attracted towards the loop and undergoes a reaction (energetically-favourable according to Frank's rule) with the upper side of the loop to form a ½[11$\bar{1}$] segment (Fig.4(a2)). This reaction segment propagates across the loop surface (Fig.4(a3)), converting $\boldsymbol{b}_L$ to ½[111], so that the loop is incorporated in the dislocation line as a set of superjogs (Fig.4(a4)). The superjogs rearrange into a U-shape with segments aligned along <112> directions and the dislocation continues to glide.

b) The dislocation is initially attracted towards the loop to form a short ½[11$\bar{1}$] reaction segment (Fig.4(b2)) with one of the [1$\bar{1}$0] loop sides direction perpendicular to the DGP. $\boldsymbol{b}_L$ of the larger part of the loop then converts into ½[1$\bar{1}$1] orientation, resulting in the configuration shown in Fig.4(b3). The latter consists of a set of edge and screw segments (labeled ½[…]s in Fig.4(b3)) connecting two arms of the edge dislocation. The newly-created screw segments, formed by splitting of the [010] segment, glide across the loop surface removing the [001] segment and

forming the configuration shown in Fig.4(b4). The latter is incorporated on the edge dislocation as a set of glissile ½[111] superjogs (see Fig.4(b5)).
The critical stress, τ_C, and the fraction of interstitials absorbed in the reactions above depend on loop size and T (and presumably on $\dot{\gamma}$, but this has not been studied as yet). The size-dependence of τ_C for the reaction in Fig.4(a) for T=300K and $\dot{\gamma}=10^7 s^{-1}$ is shown in Fig.1(a). τ_C increases linearly with the D to reach 470MPa for the largest size considered (7nm), which is close to the value for the ½[1$\bar{1}$1] DL of 8.5nm size. (Both of these loops contain approximately the same number ~1225 of SIAs.) However, despite the same critical stress, the [001] loop was completely absorbed in the simulations whereas the ½[1$\bar{1}$1] loop was not.

The T-dependence of τ_C for the reaction at $\dot{\gamma}=10^7 s^{-1}$ with the [001] loop of 3nm size shown in Fig.4(a) is presented in Fig.1(b), where τ_C is seen to reduce from 560MPa at T=0K (static simulations) to 70MPa at 300K. Further increase of T to 600K does not change τ_C. Complete absorption of the loop was observed in reactions modelled above 100K. Below 100K, the formation and glide of relatively long screw segments occurs, as in the cases above for loops having $\boldsymbol{b}_L$ = ½[1$\bar{1}$1] or ½[11$\bar{1}$]. The dislocation-DL configurations just before glide of the screw arms at τ_C are compared in Fig.2 for the ½[1$\bar{1}$1] and [001] loops (each containing 169-SIAs, simulated at 0K). Thus, in low-T simulations, release of the dislocation is controlled by glide of the screw dipole segments, which occurs prior to motion of the ½<111> reaction segment, which also controls absorption. Hence, the mechanisms of absorption are similar for the ½<111> and <100> dislocation loops. We note, however, that the stress at which a ½<111> reaction segment glides over <100> DL surface may be significantly different from that at which a <100> segment glides over a ½<111> loop.

4. Concluding remarks

The simulation of reactions between edge dislocations and dislocation loops with $\boldsymbol{b}_L$=1/2<111> or <100> has shown the following.
(i) Small loops (with size up to ~1nm) are easily absorbed by reaction with edge dislocations, independently of their Burgers vector.
(ii) Large loops are strong obstacles and, depending on the difference in orientation of the dislocation and loop Burgers vectors, are either completely or partially absorbed. The critical stress and reaction product depend on T and are controlled by the mobility of either the dislocation segment formed by a favourable DL-dislocation reaction or screw dislocations in a dipole drawn out on the pinned dislocation.
(iii) In general, the mechanism that provides complete absorption of relatively large loops involves propagation of the reaction segment over the loop surface. This motion is controlled by cross-slip of the screw dislocations formed in a dipole and can involve complicated dislocation reactions. (Examples of different reactions can be found in [9].)
(iv) Thus, thermally-activated glide and/or decomposition of the pinning segment formed in the favourable reaction determines both the absorption and critical stress, and therefore depends on temperature, strain rate and loop size.

(v) Irrespective of whether loop absorption on the dislocation is complete or not, the absorbed interstitials form a set of glissile ½<111> superjogs, so that after unpinning the edge dislocation moves under approximately the same stress as a perfect straight dislocation.

Acknowledgements

This work was performed in the framework of the 7th Framework Programme collaborative project GETMAT, partially supported by the European Commission, grant agreement number 212175.

References:

[1] S.J. Zinkle and B.N. Singh, J. Nucl. Mater. **351** (2006) 269.
[2] A.C. Nicol, M.L. Jenkins and M.A. Kirk, MRS Symp. Proc. **650** (2001) R.1.3.1.
[3] M. Victoria, N. Baluc, C. Bailat, et al. J. Nucl. Mater. **276** (2000) 114.
[4] Yu.N. Osetsky and D.J. Bacon, Model. Simul. Mater. Sci. Eng. **11** (2003) 427.
[5] A. Nomoto, N. Soneda, A. Takahashi and S. Ishino, Materials Transactions **46** (2005) 463.
[6] Z. Rong, Yu.N. Osetsky and D.J. Bacon, Phil. Mag. **85** (2005) 1473.
[7] D.J. Bacon, Yu.N. Osetsky and Z. Rong, Phil. Mag. **86** (2006) 3921.
[8] D. Terentyev, L. Malerba, D.J. Bacon and Yu.N. Osetsky, J. Phys.: Condens Matter **19** (2007) 13.
[9] D.A. Terentyev, P. Grammatikopoulos, D.J. Bacon and Yu.N. Osetsky, Acta Mat. (2008) submitted.
[10] G.J. Ackland, M.I. Mendelev, D.J. Srolovitz, D. Han and A.V. Barashev, J. Phys: Condens. Matter **16** (2004) 1.
[11] D. Hull and D.J. Bacon, Introduction to Dislocations, 4th edition, Oxford: Butterworth-Heinemann (2001).

Determination of the Activation Energy of Dislocation-defect Interactions in Molecular Dynamics Simulations

Ghiath Monnet[1], Yuri Osetsky[2] and David J. Bacon[3]

1) **EDF – R&D, Department MMC, av des Renardières, 77818 Moret sur Loing, France. Email : ghiathmonnet@yahoo.fr**
2) **Computer Science and Mathematics Division, ORNL, Oak Ridge, TN 37831, USA. Email : osetskiyyn@ornl.gov**
3) **Materials Science and Engineering, Department of Engineering, The University of Liverpool, Liverpool L69 3GH, UK. Email : djbacon@liverpool.ac.uk**

ABSTRACT

Given the time and length scales in Molecular Dynamics (MD) simulations of dislocation-defect interactions [1], MD results cannot be used directly in larger scale simulations or compared to experiment [2]. A method is proposed here to extract from MD simulations the interaction energy [3], the critical stress and the activation energy of the dislocation-void interaction. It is first shown how the critical stress can be defined and evaluated in the steady-state condition as a function of temperature. The critical stress is found to deviate from the maximum stress measured in MD simulations with increasing temperature. Also, it is shown how the time integration of the mechanical work, as well as the calculation of the critical stress at a given temperature, is enough to provide ~~to~~ a good approximation for the activation energy involved in the process. We present a method to be used in order to account for these atomic-level results in Dislocation Dynamics (DD) simulation. DD results show that it is possible to reproduce exactly the interaction strength computed from MD simulations. At finite temperature, thermal activation induces a stochastic feature of the dislocation-void interaction.

[1] Osetsky YuN, Bacon DJ, Mohles V. Phil Mag **83**, 3623 (2003)
[2] Domain C, Monnet G. Phys Rev Lett, **95**, 215506 (2005)
[3] Monnet G, Acta Mater. **55**, 5081 (2007)

This work is partially funded by the European project PERFECT (FI60-CT-2003-208840).

Molecular Dynamic Study of Screw Dislocation – Irradiation Defect Interactions

Christophe Domain, Ghiath Monnet

EDF-R&D Département MMC, Les renardières, F-77818 Moret sur Loing Cédex, France, (E-mails: christophe.domain@edf.fr, ghiath.monnet@edf.fr)

ABSTRACT

Under neutron irradiation, a hardening of the pressure vessel steels is observed due to the formation of point defect clusters and solute clusters. In order to model the plasticity of Fe alloys under irradiation a multiscale approach combining molecular dynamics and dislocation dynamics has been developed. The interaction of irradiation defects with screw dislocations is characterised by molecular dynamics as a function of temperature. The methodology used has been validated for the CRSS in pure Fe; and the potential used has been compared to some ab initio data. Results related to vacancy clusters, copper clusters and interstitial dislocation loops will be presented and discussed.

This work has been performed within the European PERFECT project (FI6O-CT-2003-508840) which has sponsored this study.

Object kinetic Monte Carlo study of the sink strength of dislocations

Lorenzo Malerba[1], Charlotte Becquart[2], Christophe Domain[3]

[1] Institute of Nuclear Materials Science, SCK•CEN, Boeretang 200, 2400 Mol, Belgium, lmalerba@sckcen.be; [2]Laboratoire de Métallurgie Physique et Génie des Matériaux, UMR 8517, Université Lille-1, 59655 Villeneuve d'Ascq Cédex, France, charlotte.becquart@univ-lille1.fr; [3]EDF-R&D Département MMC, Les Renardières, 77818 Moret sur Loing Cédex, France, christophe.domain@edf.fr

ABSTRACT

We study the sink strength for three-dimensionally (3D) versus one-dimensionally (1D), or mixed 1D/3D, migrating defects in the case of an ordered array of straight dislocations , using object kinetic Monte Carlo (OKMC) techniques. We show that the “master curve” approach, that describes the sink strength transition from fully 3D to purely 1D migration regime, is extendable to dislocations, although further theoretical developments are required.

1. Introduction

The sink strength for three-dimensionally (3D) versus one-dimensionally (1D), or mixed 1D/3D, migrating defects in irradiated materials has recently attracted much attention, as many experimental observations cannot be interpreted unless 1D or mixed 1D/3D migration patterns are assumed for self-interstitial atom clusters produced in displacement cascades. Analytical expressions for the sink strengths for defects migrating in 3D and also 1D have been hence developed and a "master curve" approach has been proposed to describe the transition from 1D to 3D regime in the case of spherical absorbers (SA) [1]. Object kinetic Monte Carlo (OKMC) methods have been then used to corroborate the theoretical expressions, in a wide range of volume fractions, for different migration patterns [2]. This technique has been shown to reproduce the theoretical expressions of the sink strengths of SA in the whole range, to support the “master curve” approach and to be sensitive enough to suggest corrected expressions for large sink volume fractions. Here we extend the study to the case of an ordered array of straight dislocations. We show that the “master curve” approach seems to be extendable to dislocations, too. Based on the comparison with OKMC results, we briefly discuss advantages and limitations of the expressions and the OKMC technique itself.

2. Method

We have estimated the sink strength of a straight dislocation using the same method as in [2], having in mind bcc iron as reference material. The 3D to 1D regime transition was explored by

increasing the number of 1D jumps after which the defect changes direction, n_{ch}. In addition, the 1D limit was also simulated by requiring 2 eV of energy for change of direction at 573 K, which corresponds in practice to no change of direction in the course of the whole simulation (the effectiveness of this way of operating to reach the 1D limit, using a non-cubic box, is demonstrated and discussed in [2]). Statistical significance was ensured by following the histories of about 30000 defects in each case. The straight dislocation was simulated as a cylinder whose two opposite faces touch the faces of a non-cubic simulation box. Since no defect can ever impinge on the cylinder from outside the box, this is an effective way to simulate an infinitely long straight dislocation. Due to periodic boundary conditions, this corresponds to simulating a regular array of parallel dislocations. Different dislocation densities, ρ_d (between 10^{14} and 10^{15} m^{-2}), and capture radii, r_c (between 2 and 9 nm), were considered.

3. Results

3.1 3D and 1D limits

The theoretical expression for the sink strength for 3D migrating defects deduced by Wiedersich in the case of a regular array of parallel straight dislocations, as reported by Nichols [3], is:

$$k_{d,3}^2 = \frac{2\pi(1-\rho^2)}{\ln(1/\rho)-\frac{3}{4}+\frac{1}{4}\rho^2(4-\rho^2)}\rho_d \quad (1)$$

where $\rho = r_c(\pi\rho_d)^{1/2}$. The results obtained in our simulations when setting n_{ch}=1 match perfectly those obtained from Eqn. (1). In the case of 1D migrating defects, the theoretical expression is the one proposed in [4]:

$$k_{d,1}^2 = 3 \times 2(\pi r_c \rho^*), \quad (2)$$

where the factor 3 allows for the use, here, of the 3D diffusion coefficient and ρ^* is the mean number of dislocations lines intersecting a unit area (surface density: in the present case of regular array of parallel dislocations, $\rho^*=\rho_d$). The results obtained in our simulations when setting n_{ch} to very high values (up to 10^{11}) or by requiring an energy for change of direction of 2 eV match reasonably well those obtained from Eqn. 2.

3.2 Transition from 3D to 1D regime

In Fig. 1 the 3D to 1D transition of the sink strength is shown for a few capture radii (from 2.25 to 6.25 nm), with $\rho_d=10^{15}$ m^{-2}, as a function of the length before change of direction, $l_{ch}=b\sqrt{n_{ch}}$ (b is the jump length, i.e. the 1st nearest neighbour distance in bcc iron). The transition from 3D to 1D regime occurs quite abruptly, as compared to the case of SA [2]: for a length before change of direction of ~250 nm the 1D regime is already effectively reached.

This abrupt transition is reflected in the corresponding master curve representation, given in Fig. 2 for all the studied conditions. Here, the simulation results were used to calculate x and y as (no lateral translation is considered in the present study) [1]:

$$x^2 = \frac{\left(k_{d,3}^2/k_{d,1}^2\right)\left[\left(k_{d,3}^2/k_{d,1}^2\right)-1\right]}{\left(l_{ch}^2 k_{d,3}^4/12k_{d,1}^2\right)+1} \qquad y = \frac{k_{d,lch}^2}{k_{d,1}^2} \tag{3}$$

where $k_{d,lch}^2$ is the sink strength for a given l_{ch} and all sink strengths in the equation refer to the same choice of capture radius and dislocation density. In the same figure, the master curve expressed as [1]

$$y = \frac{1}{2}\left(1+\sqrt{1+4x^2}\right) \tag{4}$$

is traced. This curve (Eqn. 4) reproduces well the simulation points in the 1D and 3D limit regions, but the abrupt 3D to 1D transition causes a discrepancy to appear.

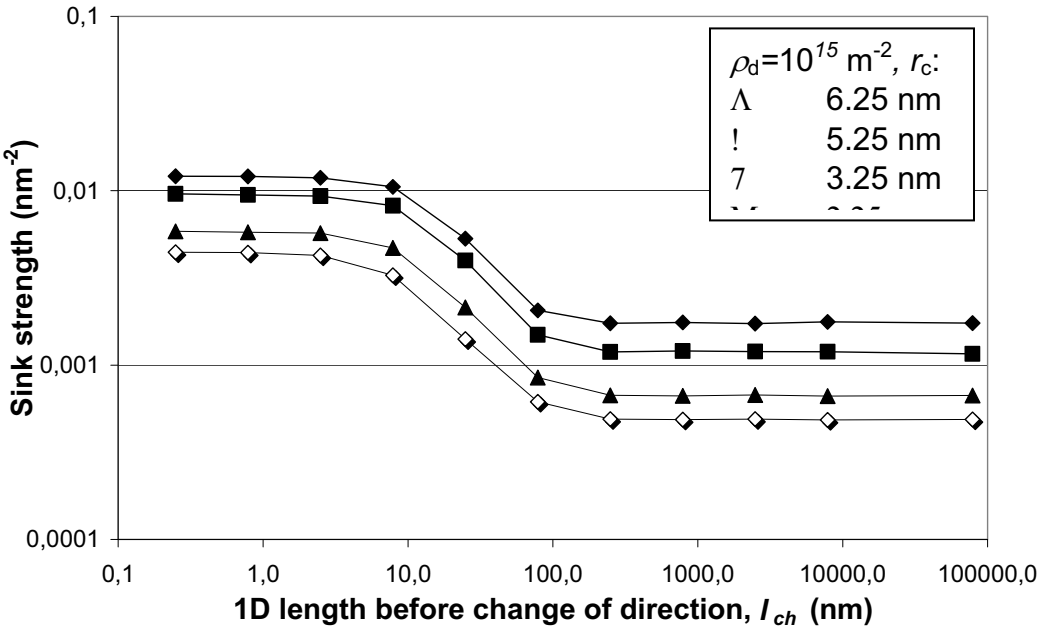

Figure 1. 3D to 1D transition of the sink strength versus length before change of direction.

4. Concluding remarks

Eqns. 3 and 4 are stated to be valid for any type of sink [1] and indeed a relatively good agreement between the master curve and the simulation data points is found. However, the 3D-1D regime transition in the present case of dislocations is observed to be more abrupt than in the previously addressed case of SA and this does not seem to be grasped by Eqns. 3 and 4, which are, however, proven to work for SA [2]. It is therefore believed that some small correction

should be introduced in the theoretical expression to explicitly allow for the specificity of dislocation type sinks.

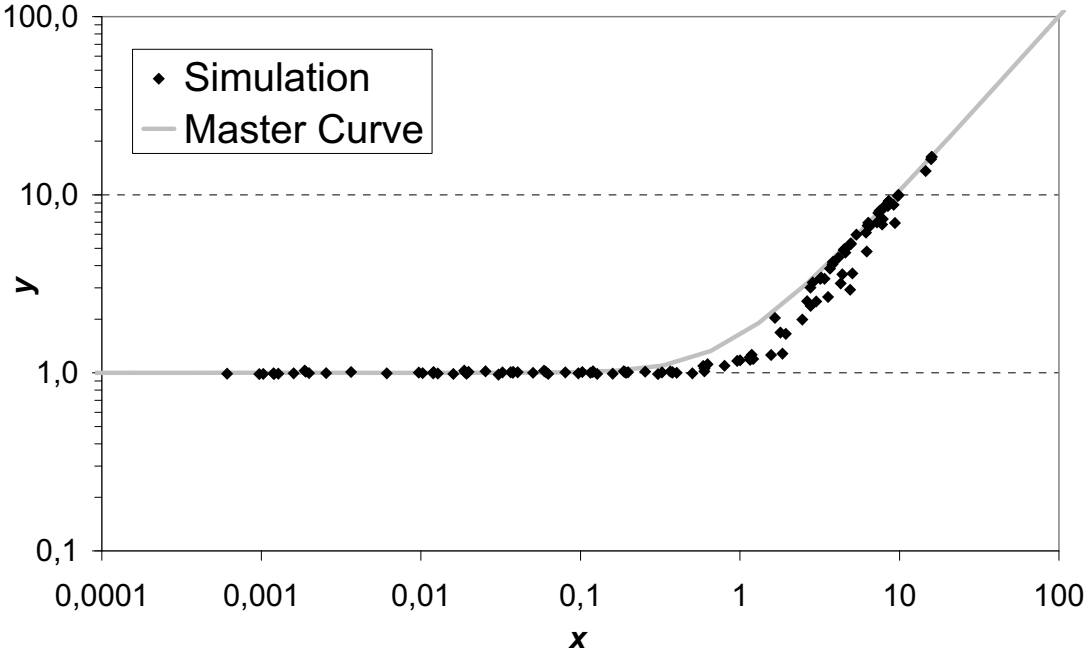

Figure 2. Comparison between simulation data points and master curve.

Even if a better agreement was reached, however, the main limitation of the present study is that only ordered arrays of straight dislocations are considered. This situation is far from being real. However, reliable theoretical expressions for the sink strengths of randomly oriented and distributed dislocation do not exist [5]. *A priori* a random distribution of dislocations could be introduced in the simulation volume where OKMC simulations are performed. However, for the distribution to be realistic, the size of the simulation volume should be too large to be feasible with present-day computers. Alternatively, more complex advanced algorithms should be developed and implemented.

Acknowledgements

The authors gratefully acknowledge useful discussions of these results with S. Golubov.

References

[1] H. Trinkaus, H.L. Heinisch, A.V. Barashev, S.I. Golubov, and B.N. Singh, Physical Review B, **66,** 060105 (2002) and refs. therein; H. Trinkaus, B.N. Singh, and S.I. Golubov, Proceedings MMM-2 Conference, Ed. N.M. Ghoniem, (2004, Los Angeles, CA).
[2] L. Malerba, C.S. Becquart, and C. Domain, Journal of Nuclear Materials, **360,** 159 (2007).
[3] F.A. Nichols, Journal of Nuclear Materials, **75**, 32 (1978).
[4] A.V. Barashev, S. Golubov, and H. Trinkaus, Philosophical Magazine A, **81**, 2515 (2001).
[5] A. D. Brailsford and R. Boullough, Philosophical Transactions Royal Society London, **302**, 87 (1981).

A modelling study of the relationship between primary damage features and the long term defects clusters growth

Marc Hou[1], Abdelkader Souidi[2], Charlotte S. Becquart[3], Christophe Domain[4], Lorenzo Malerba[5]

[1]Physique des Solides Irradiés et des Nanostructures CP234, Université Libre de Bruxelles, Bd du Triomphe, B-1050 Bruxelles, Belgium (E-mail : mhou@ulb.ac.be)
[2]Centre Universitaire Dr. Moulay Tahar de Saida, BP138 En Nasr, Saida 20000, Algeria (E-mail : aek_souidi@yahoo.fr)
[3]Laboratoire de Métallurgie Physique et Génie des Matériaux, UMR 8517, Université Lille-1, F-59655 Villeneuve d'Ascq Cédex, France (E-mail : charlotte.becquart@univ-lille1.fr)
[4]EDF-R&D Département MMC, Les renardières, F-77818 Moret sur Loing Cédex, France, (E-mail : Christophe.domain@edf.fr)
[5]SCK•CEN, Reactor Materials Research Unit, B-2400 Mol, Belgium, (E-mail: lorenzo.malerba@sckcen.be)

ABSTRACT

In a previous work [1], the fraction of primary point defect clusters and their spatial correlations were singled out as of prime importance in the long term point defect cluster growth while many others were found irrelevant. In this report, we study correlations in more detail. It is suggested that the knowledge of the spatial confinement of displacement cascades may be sufficient to predict cluster size distributions on the long term. This study is based on extended Object Kinetic Monte Carlo simulations with the LAKIMOCA code with four different parameterizations and using cascades generated with the MOLDY code at ORNL

[1] M. Hou, A. Souidi, C.S. Becquart, C. Domain, L. Malerba ; J . Nucl. Mater., in press.

This work was prepared in the framework of the integrated project PERFECT (F160-CT-2003-508840) under program EURATOM FP-6 of the European Commission.

On the role of helical turns in the formation of clear bands in irradiated materials

David Rodney[1], Thomas Nogaret[1], Marc Fivel[2]

[1]INP Grenoble, Domaine Universitaire BP 46, , Saint Martin d Heres, 0 F38402, (E-mails: david.rodney@simap.grenoble-inp.fr, thomas_nogaret@brown.edu)
[2]CNRS, France (E-mail: marc.fivel@simap.grenoble-inp.fr)

ABSTRACT

The plastic deformation of irradiated metals is localized in shear bands that appear post-mortem in TEM as empty of irradiation defects and are thus called clear bands. We analyzed the mechanisms of clear band formation using a multi-scale simulation approach based on a combination of Molecular Dynamics (MD) and Dislocation Dynamics (DD) simulations. The MD simulations were used to study the elementary interactions between edge/screw dislocations and irradiation defects in the form of interstitial Frank loops. These simulations showed that defect unfaulting and absorption occurs mainly via screw dislocations that acquire Helical Turns. On the other hand, edge dislocations mainly shear faulted defects and drag away unfaulted defects in the form of glissile jogs. These elementary mechanisms were introduced in a DD code to simulate the expansion of a dislocation pile-up in a population of irradiation defects. These simulations confirm the dominant role played by helical turns in the clearing and broadening of clear bands.

Dynamics of dislocation-localized obstacle interaction: what can we learn from atomic level modelling

Yuri Osetsky

**ORNL, One Bethel Valley Rd, P.O.Box 2008, MS-6138,
Oak Ridge, TN 37831, USA (E-mail: osetskiyyn@ornl.gov)**

ABSTRACT

Development of models for investigation of mechanical properties requires understanding of the phenomena involved at both the atomic and continuum levels. This paper concentrates on the former level, and describes the application of a model developed recently to study the motion of an initially straight edge and screw dislocations through a row of localized obstacles (voids, coherent precipitates or stacking fault tetrahedra in alpha-iron and copper). The model can provide quantitative information on the stress–strain relationship, energy barrier profile and strength characteristics for dislocation–obstacle interaction, and the effects of stress, strain rate and temperature on the process can be investigated. New results on data and atomic-scale mechanisms associated with strengthening due to voids and precipitates over a range of size are presented and compared with earlier continuum treatments. It is shown that atomic-level simulation is essential for revealing information required for multiscale modelling of phenomena in radiation damage.

Dislocation interaction with C in alpha-Fe: a comparison between atomic simulations and elasticity theory

Emmanuel Clouet[1], Sébastien Garruchet[2], Hoang Nguyen[3], Michel Perez[2], Charlotte Becquart[3]

[1]SRMP, CEA Saclay, , Gif-sur-Yvette, 91191 (E-mail : emmanuel.clouet@cea.fr)
[2]MATEIS, INSA Lyon, France, 25 avenue Capelle, Villeurbanne, 69621,
[3]LMPGM, Université de Lille, France

ABSTRACT

The interaction of C atoms with a screw and an edge dislocation is modelled at an atomic scale using an empirical Fe-C potential based on the Embedded Atom Method (EAM) and molecular statics simulations. Results of atomic simulations are compared with predictions of elasticity theory. At this scale, the C interstitial atom is modeled as an elastic dipole interacting with the Volterra elastic field created by the dislocation. It is shown that a quantitative agreement can be obtained between both modelling techniques as long as anisotropy is included in elastic calculations and both the dilatation and the tetragonal distortion induced by the C interstitial are considered [1]. The comparison shows that elastic calculations remain valid even when the C atom gets really close to the dislocation core. Using isotropic instead of anisotropic elasticity only allows to predict the main trends of the interaction. Considering the dilatation of the C interstitial and neglecting its tetragonal distortion lead to a wrong interaction. [1] E. Clouet, S. Garruchet, H. Nguyen, M. Perez and C.S. Becquart, Acta Mater. submitted (2008).

Computer Simulation of Effects of PKA Nature on Cascade Damage in Iron

Andy Calder[1], David Bacon[1], Sasha Barashev[1], Yuri Osetsky[2]

[1]University of Liverpool, Department of Engineering, Merseyside L69 3GH, Liverpool UK, (E-mails: afcalder@liv.ac.uk, djbacon@liv.ac.uk, a.barashev@liv.ac.uk);
[2]Computer Science and Mathematics Division, Oak Ridge National Laboratory, One Bethel Valley Rd, P.O.Box 2008, MS-6138, Oak Ridge, TN 37831, (E-mail: osetskiyyn@ornl.gov)

ABSTRACT

TEM observations of ion-irradiated thin foils of iron have shown that the probability of formation of visible damage in the core of displacement cascades is sensitive to the mass and polyatomic nature of the incident ions (e.g. Jenkins et al., Phil. Mag. A 37 (1978)). Whereas vacancy dislocation loops are seen only after self-ion (Fe^+) irradiation at dose levels when cascade overlap is significant, heavy ions such as W^+ and molecular Sb^{2+} produce measurable defect yield at smaller doses due to collapse of individual cascades. However, it has been argued from the evidence of MD simulations that the proximity of a foil surface has a strong influence on the collapse process in TEM foils (e.g. Ghaly et al., Phil. Mag. A 79 (1999)). Thus, the present MD study investigates the effect of primary knock-on atom (PKA) mass and nature on cascade damage in the bulk of a model representing BCC iron. Atoms simulating PKAs of C, Fe, Bi, Bi_2 and Bi_3 with energy in the range 5 to 30keV have been considered. This choice produces a matrix of PKA conditions, namely increasing energy at constant mass, increasing mass at constant energy and constant energy per PKA. It is found that the nature of the PKA has a major effect on the form of cascade damage. Increasing the mass of single-atom PKAs increases the yield of defect clusters in the form of dislocation loops. For example, interstitial loops of ½<111> type and both vacancy and interstitial loops of <100> type are formed at higher energy, the latter being observed in MD simulation for the first time. The efficiency of production of large clusters is increased further in cascades created by di- and tri-atomic knock-on events. There is also a correlation between production of large vacancy and interstitial clusters in the same cascade.

Defect Production in Iron: Review of Atomistic Simulations

Roger E. Stoller

Oak Ridge National Laboratory
Materials Science and Technology Division, P. O. Box 2008, MS-6138
Oak Ridge, TN 37831-6138, USA
(E-mail: rkn@ornl.gov)

ABSTRACT

The results of an extensive investigation of primary damage formation in iron using molecular dynamics (MD) displacement cascade simulations in iron will be presented. These simulations have been carried out over several years, leading to the development of a substantial cascade database that includes cascade simulations energies from near the displacement threshold (~100 eV) to 200 keV. The temperature range of the simulation database is 100 to 900K. The review will focus on analyzing the role of cascade energy and temperature in primary damage formation. Damage production is characterized in terms of the total number of point defects (interstitials and vacancies) produced, the partitioning of the this total into isolated and clustered defects, and the size distributions of the interstitial and vacancy clusters. Although most of the data base consists of cascades produced in perfect single-grained material, the impact of pre-existing damage, free surfaces, and fine grain size has also been evaluated for a limited number of conditions. The applicability of the atomistic simulations for use in providing appropriately-averaged primary damage parameters for use in kinetic models will also be discussed.

Research sponsored by the Division of Materials Sciences and Engineering and the Office of Fusion Energy Sciences, U.S. Department of Energy, under contract DE-AC05-00OR22725 with UT-Battelle, LLC.

Decoration of Edge Dislocation with Interstitial Clusters Under Neutron Irradiation

Alexander V. Barashev[1], Stanislav I. Golubov[2,3], David J. Bacon[1], Yury N. Osetsky[2], Roger E. Stoller[2]

[1]Department of Engineering, The University of Liverpool, Brownlow Hill, Liverpool, L69 3GH, UK (E-mails: a.barashev@liv.ac.uk, djbacon@liv.ac.uk); [2]Materials Science and Technology Division, ORNL, Oak Ridge, TN 37831-6138, USA (E-mails: 6gs@ornl.gov (S.I.G.), osetskiyyn@ornl.gov (Yu.N.O.), rkn@ornl.gov (R.E.S.); [3]Center for Materials Processing, University of Tennessee, East Stadium Hall, Knoxville, TN 37996-0750, USA.

ABSTRACT

The decoration of dislocations with clusters of interstitial atoms is one of the key processes that control damage accumulation and affect the ductility of metallic materials under neutron irradiation in nuclear reactors. Application of the kinetic Monte Carlo in its conventional form to simulate this process is impossible due to the presence of a wide range of characteristic times. In this paper, a Monte Carlo model is formulated for the first time, which is capable of studying the process on a required time-scale. It is based on an analytical analysis and results of smaller scale Monte Carlo calculations. It is shown for the first time that a key process in decoration formation is the thermally activated dissociations of interstitial clusters from dislocations. The distribution of the cluster Burgers vector directions and the effect of mutual interactions between clusters is studied. An explanation of the irradiation dose dependence of the decoration observed in experiments is proposed.

A.V.B. acknowledges a research grant from the UK Engineering and Physical Sciences Research Council. Research at ORNL was sponsored by the Division on Materials Sciences and Engineering (R.E.S. and Y.N.O.) and the Office of Fusion Energy Sciences (S.I.G.), U. S. Department of Energy, under contract no. DE-AC05-00OR22725 with UT-Battelle, LLC.

Point defects in Zirconium and their influence on radiation damage

Petrica Gasca[1], Christophe Domain[2], Alexandre Legris[1]

[1]LMPGM-USTL, USTL Bat C6, Villeneuve D'Ascq, 59655,
(E-mails : petricag@gmail.com, alexandre.legris@univ-lille1.fr);
[2]MMC EDF R&D, Les Renardieres, Moret sur Loing, F-77250,
(E-mail : christophe.domain@edf.fr)

ABSTRACT

The cladding material in Pressure Water Reactors is made with zirconium alloys that are submitted to intense neutron radiation damage in service conditions. As a consequence, the formation of dislocation loops evenly distributed in the basal and prismatic planes induce an elongation of the textured material. To understand the growth and more generally the microstructure evolution under irradiation it is crucial to know the structure and mobility of point defects which are produced in amounts orders of magnitude above their thermal equilibrium values. The present work presents an exhaustive ab initio study of point defects in zirconium including self-interstitials and vacancies. The defects were characterized (formation energy and volume) and their mobility was determined using kinetic Monte Carlo, allowing to estimate the diffusion coefficient of both interstitials and vacancies. The results are at-odds with previous estimation based on empirical potentials since self-interstitials have a rather isotropic migration while vacancies move faster in the basal planes.

Core Structure, Peierls Potential and Kinks of Screw Dislocations in Iron from First Principles

Lisa Ventelon, Francois Willaime, Emmanuel Clouet

**Service de Recherches de Metallurgie Physique, CEA/Saclay,
Gif-sur-Yvette, 91191 France,
(E-mails : lisa.ventelon@cea.fr, francois.willaime@cea.fr, emmanuel.clouet@cea.fr)**

ABSTRACT

A quantitative description of straight and kinked <111> screw dislocations in iron from first principles is presented. The calculations are carried out within the density functional theory (DFT) framework using the SIESTA code and simulation cells containing up to 800 atoms. The construction of simulation cells appropriate for such extended defects has been optimized for cell sizes accessible to DFT calculations. We have rationalized the cell-size dependences of the energetics evidenced both in the cluster approach and in the dipole approach for various cell and dipole vectors; they are due respectively to surface-dislocation and core-core interactions. It is concluded that a quadrupolar arrangement of dislocation dipoles is best suited for such calculations. In agreement with previous DFT calculations in body centered cubic transition metals, a non- degenerate structure is found for the core. From a detailed comparison with anisotropic elasticity a significant dilation effect has been evidenced in addition to the Volterra field. Two high symmetry directions of the Peierls potential have been sampled: the line joining two easy-core positions – which gives the Peierls barrier – and that from an easy to a hard-core position. The behavior of the Ackland-Mendelev potential for iron, which gives the correct non-degenerate core structure unlike most other potentials, has been tested against the present results. It compares well with the DFT -surfaces but discrepancies appear on the deviation results for the from anisotropic elasticity of the edge component and on the Peierls potential: it underestimates the Peierls energy by a factor of three and overestimates the energy difference between easy and hard cores by a factor of five, and it yields a double-hump Peierls barrier instead of a single hump one within DFT. Attempts to improve this potential will be presented. Finally, the structure and the formation and migration energies of single kinks have been investigated. The methodology for constructing triperiodic cells with a single kink on each dislocation line has been developed. Results obtained with empirical potentials as well as preliminary DFT calculations are presented. The two types of kinks – left and right – are found to have significantly different formation energies.

Mechanisms Operating during Plastic Deformation of Metals

Helmut Trinkaus[1], B.N. Singh[2], S.I. Golubov[3]

[1]Institut für Festkörperforschung, Forschungszentrum Jülich, D-52425 Jülich, Germany, (E-mail: h.trinkaus@fz-juelich.de)
[2]Materials Research Department, Risø National Laboratory for Sustainable Energy, Technical University of Denmark, P.O. Box 49, DK-4000 Roskilde, Denmark, [3]Materials Science & Technology Division , Oak Ridge National Laboratory, P.O. Box 2008, Oak Ridge, TN 37831-6376, USA

ABSTRACT

Recent in-reactor tensile tests (IRTs) on pure Cu have revealed a deformation behaviour which is significantly different from that observed in post-irradiation tensile tests (PITs). In IRTs, the material deforms uniformly and homogeneously without yield drop and plastic instability as commonly observed in PITs. An increase in the pre-yield dose results in an increase in the level of hardening over the whole test periods and a decrease in the uniform elongation suggesting that the materials "remember" the impact of the pre-yield damage level. These features are modelled in terms of the decoration of dislocations with glissile dislocation loops. During pre-yield irradiation, dislocation decoration is due to the one-dimensionally (1D) diffusion of cascade induced self-interstitial (SIA) clusters and their trapping in the stress field of the static dislocations. During post-yield irradiation and deformation, moving dislocations are decorated by the sweeping of matrix loops. The interaction of dislocations with loops and between loops is discussed as a function of the relevant parameters. On this basis, the kinetics of decoration is treated in terms of fluxes of loops to and reactions in a conceived 2D space of decoration. In this space, coalescence, alignment and mutual blocking reactions are characterised by appropriate reaction cross sections. In the kinetic equations for "dynamic decoration" under deformation, the evolution of the dislocation density is taken into account. Simple solutions of the kinetic equations are discussed. The origin of the apparent memory of the system for the pre-yield dose is identified to be due to the concurrent evolution of the dislocation density with effectively similar rates during the transients of both processes. The contributions of dislocation decoration to yield and flow stresses is attributed to the interaction of dislocations with aligned loops temporarily or permanently immobilized by other loops or SFTs ("decoration enhanced obstacle hardening"). On this basis, the yield and flow stress are discussed as a function of pre-yield dose, post-yield dose and strain, respectively. Assuming physically reasonable values for the parameters involved we are able reproduce the general trends and the right orders of magnitude of the yield and flow stresses of Cu measured in the IRTs.

On the role of elastic strains in the precipitation of second phases

Volker Mohles, Emmanuel Jannot, Günter Gottstein

IMM, RWTH Aachen University, Kopernikusstr. 14, Aachen, Germany D-52056, (E-mails: mohles@imm.rwth-aachen.de, jannot@imm.rwth-aachen.de, gg@imm.rwth-aachen.de)

ABSTRACT

The use of Green functions allows the efficient resolution of elasticity problems in Monte-Carlo simulations. However, previous attempts to use this methodology to derive the stored elastic energy in a solid solution haven't been fully successful. For example, the one atom thick plate morphology of GP zones in Al-Cu alloys can't be reproduced using the theory developed by Khachaturyan or Cook-de Fontaine. The present work provides an explanation for this discrepancy. An improved version of the Microscopic Elasticity theory is presented in which the nature of the target atom for the Kanzaki force is considered. Calculations indicate that this improvement reduces the error generated by the use of Green functions to less than 2% compared to Molecular Statics relaxations. Consequently, the role of elastic strains for the precipitation of second phases can be evaluated more precisely. Simulations for model materials revealed that elastic strains should be first considered as a positive driving force for nucleation. For example, the energy gain offered by the concentration of point defects like solute atoms can explain the stability of second phases up to the melting point of aluminum for solute atoms having a 10% lattice mismatch. Using the improved theory, new insight on the factors explaining the precipitate morphology is provided. This work confirms the importance to consider elastic anisotropy.

Substitutional Al solute interaction with edge and screw dislocation in Ni: a comparison between atomistic computation and continuum elastic theory

S. Patinet[1]

[1]**Service de Recherches de Métallurgie Physique, CEA-Saclay/DEN/DMN**
91191 Gif-sur-Yvette Cedex, France, www.cea.fr

ABSTRACT

Molecular static simulations have been performed to study the interaction between a single dislocation and a substitutional Al solute atom in a pure crystal of Ni. When the Al solute is situated at intermediate distance from the slip plane, we find that both edge and screw dislocations experiment a non-negligible binding energy. We show that for such length scale the description of the elasticity theory can be improved by taking into account the spreading of dislocation cores via the Peierls-Nabarro model.

1. Introduction

The mechanical behaviour of metallic alloyed materials is largely caused by the interactions between dislocations and solute atoms. Foreign atoms play the role of obstacles to the dislocations motion and at finite temperatures segregate on dislocation forming Cottrell atmospheres. These atomic processes lead to phenomenon as solid solution hardening, heterogeneous precipitation, static or dynamic ageing and impact the yield stress of the alloy. Therefore, understanding the interaction between solute atoms and dislocation is an important issue in materials science. One of the most recent ways to examine this problem quantitatively is to perform atomistic simulations [1, 2]. Empirical potential based on Embedded Atom Method (EAM) have been found to be reliable to model dislocation in Face Centered Cubic (fcc) metals [1]. Recently, the role played by the screw dislocation segments have been addressed and it has been shown that for a certain model alloy, i.e. Ni(Al) the pinning strength by solutes situated in the vicinity of the core are of same order as for the edge dislocation [2, 3]. On the other hand most of the metal macroscopic behaviors involve collective evolution of dislocations and make atomistic simulations no more tractable. It is therefore interesting to tentatively model the dislocation solute interactions via a continuum elastic theory [4, 5, 6] to check its range of validity and to provide a relevant description of it that may serve at larger scale as for instance into the dislocation dynamics simulations.

2. Atomic Simulations

We perform molecular static (MS) relaxations in pure Ni to study the geometry of perfect isolated edge and screw dislocation (see Fig. 1). The calculations are done using EAM potentials supplied by [7] that gives a good description of the Ni(Al) alloy properties. The simulation cell is

oriented so as that the horizontal Z planes are the $(1\bar{1}1)$ slip plane of the fcc lattice while the Y direction corresponds to the dislocation line ($a_0/2[110]$, screw dislocation Burgers vector). The X direction is orthogonal to Z and Y and points at the dislocation motion ($a_0/2[110]$, edge dislocation Burgers vector). The simulation box sizes along the directions X, Y, Z are 100×30×50 Å and 80×20×80 Å for the edge and the screw dislocation respectively. Periodic boundary conditions are imposed along X and Y while free surface conditions are applied to the atoms in the upper and lower Z surfaces [1, 2, 3]. The relaxed crystal structure of a single perfect dislocation is shown in Fig. 1 through an analysis of the Burgers vector density of both edge and screw component lying in the slip plane. As expected in Nickel, the full dislocation dissociates into 2 Shockley partials with $a0/6[211]$ and $a0/6[12\bar{1}]$ Burgers vectors separated by a stacking fault region. The core of each partial is far from being compact and spreads in the glide plane over a finite width ξ. The dissociation distance d between partials as well the partial core widths are found larger for the edge dislocation than for the screw.

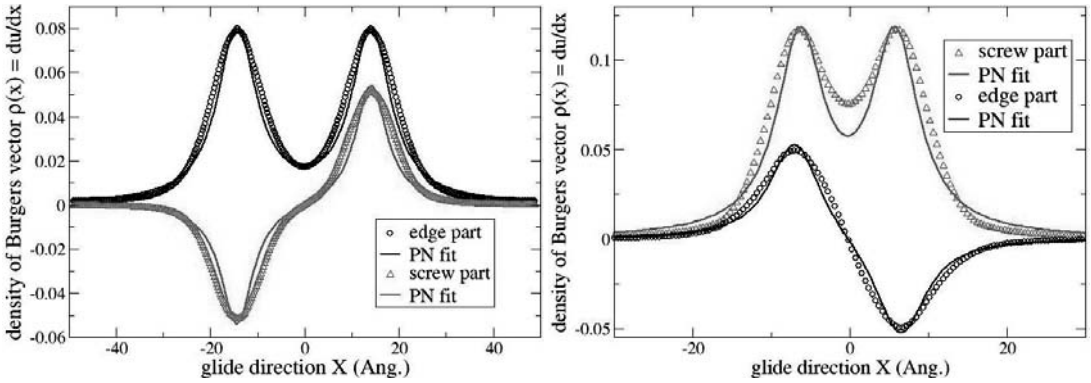

Figure 1. Densities of Burgers vectors with respect to the glide direction in the slip plane: (a) edge dislocation, (b) screw dislocation. The symbols represent the simulation data while the curves are their fits on Peierls-Nabarro displacement field.

In a second time, we carried out the same MS simulations except that a single isolated Al atom is placed in a simulation cell of pure Ni. Then an external applied shear stress is produced by imposing extra forces to the atoms in the upper and lower Z surfaces making the dislocation glide toward the obstacle. At each relaxation step a gradient algorithm forces the dislocation to explore its minimum potential energy path. The interaction energy is recorded for all relative distances between the dislocation and the Al solute atom situated at the third $[1\bar{1}1]$ plane from the glide plane for both dislocations (see Fig. 2). The minimum distance between the solute and the dislocation cores is thus about ~ 5 Å and corresponds to two and a half of the inter-plane distance along the $[1\bar{1}1]$ direction. As expected, the compressive zones, above the glide plane for the edge dislocation and alternate for each partial of the screw dislocation, are repulsive for the solute while the tensile zones are attractive since Al impurities dilate the Ni matrix. The attractive and repulsive peaks are clearly associated with the positions of the partials. At such distance the maximum interaction energy is found to be -0,046 eV for the edge dislocation while it is twice smaller for the screw. In case of the screw dislocation, the maximum binding energy is greatly increase by the modulus effect. From the results reported in Fig. 2, we can expect the segregation of solutes forming Cottrell atmospheres of different shapes for each dislocation character: below the glide plane for the edge dislocation, above the leading partial and below the trailing one for screw segments. Therefore, the interaction between screw dislocation and solute

atoms even at such length scale can not be neglected and the screw segments may as well participate in ageing phenomenon or solid solution hardening.

Table 1. Physical constants calculated from Ni(Al) EAM empirical potential.

C_{11} GPa	C_{12} GPa	C_{44} GPa	$\frac{dC_{11}}{C_{11}dc}$	$\frac{dC_{12}}{C_{12}dc}$	$\frac{dC_{44}}{C_{44}dc}$	E GPa	v	δV Å^3	d_e Å	d_s Å	ξ_e Å	ξ_s Å
246	147	125	-1,87	-1,31	-1,28	242	0,27	2,1	28,4	12,6	4,5	3,8

3. Elasticity Theory

The linear continuum elastic theory has shown to be reliable to describe the interaction energy between defects and dislocations as long as deformations are small, i.e. far enough from the dislocation core [4, 5, 6]. Considering at same time size and modulus misfits, the binding energy between a dislocation and a single defect reads as follows [1]:

$$E_b = P\delta V - \frac{1}{2} V \sigma_{ij} \frac{\partial S_{ijkl}}{\partial c} \sigma_{kl}, \tag{1}$$

where P and σ_{ij} are the hydrostatic pressure and the stress field created by the dislocation at the solute position, V is the atomic volume in the matrix, δV the solute relaxation volume, c the solute concentration and S_{ijkl} is the compliance tensor expressed in this study via isotropic constant (see Tab. 1). Since a substitutional Al atom in fcc Ni does not break the cubic symmetry of the lattice it is not required to account for tetragonal distortion effect. For our isotropic elasticity calculations, we use the Young's modulus E and the Poisson coefficient v obtained by the Voigt average. Taking full account of the periodic boundary conditions as well as the dissociation of dislocation we carried out the computations of types [8]: (i) Volterra dislocation with compact core, (ii) Peierls-Nabarro (PN) dislocation with an extended core region.

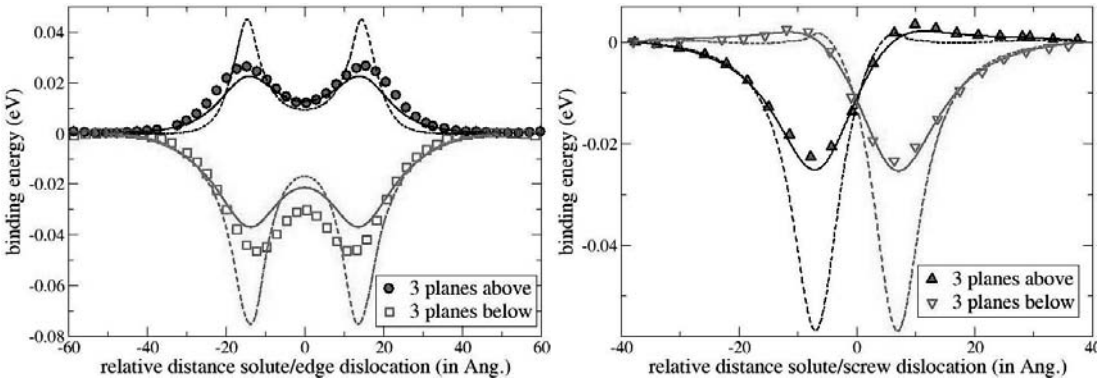

Figure 2. The binding energy between one Al solute atom and a dislocation against the distance between the dislocation and the obstacle in the glide direction: (a) edge dislocation, (b) screw dislocation. The solute is situated in the third $(1\bar{1}1)$ planes above (filled symbols) or below (open symbols) the glide plane. The curves correspond to analytical treatments: Volterra dislocation (dashed line) and Peierls-Nabarro dislocation (full line).

In Fig. 2, the predicted elasticity results are found to be in fairly good agreement with the atomistic results. However, several discrepancies need to be pointed out. Due to the singularity

of its elastic field, the results given by Volterra dislocation systematically overestimate the interacting energy just above or below the core positions of the partials [5]. On the other hand, we note that the interaction energy dependency described by a PN dislocation gives a better agreement with the simulation data. Indeed, the PN description of a spreaded core is closer from the burgers density profile of the dislocation (see Fig.1). We also remark an overestimation of the interaction energy for the edge dislocation when the solute is situated around the stacking fault region. This seems consistent since the elasticity solutions do not address, in the present study the solute–stacking fault interaction. To improve the transfer from the atomic scale to a continuous theory we emphasize that some improvements of the model would be required as the nonlinear, anisotropic nature of the dislocation-defect interaction as well as the stacking fault elastic field. Despite of simplified assumptions, the PN model has the great merit of providing an analytical nonlinear elastic model of the dislocation core. However at smaller length scales, nearby of the dislocation core, linear elastic theory breaks down and the PN model calculations deviate from our atomistic calculations.

4. Conclusions

The aim of the present paper was to extend the comparison between the atomistic computations and elastic theory in the case of a single substitutional solute atom and dislocations in a fcc alloy. For an impurity situated at intermediate distance from the glide plane, we found that the binding energy of the screw dislocation is twice smaller than the edge one. Another issue of the present paper was to tentatively apply analytical models to compute the binding energy. It has been shown that the elasticity theory manages to predict qualitatively the interaction energy and that these predictions can be improved by accounting for the spreading of the dislocation core.

References

[1] D. L. Olmsted, L. G. Hector and W. A. Curtin, “Molecular Dynamics Study of Solute Strengthening in Al/Mg Alloys”, Journal of the Mechanic and Physics of Solids, 54, 1763 (2005).
[2] L. Proville, D. Rodney, Y. Brechet and G. Martin, “Atomic-scale Study of Dislocation Glide in a Model Solid Solution“, Philosophical Magazine, **86**, 3893 (2006).
[3] S. Patinet and L. Proville, “Depinning Transition for a Screw Dislocation in a Model Solid Solution”, Physical Review B, Article in press, Accepted manuscript (2008).
[4] E. Clouet, “The Vacancy-Edge Dislocation Interaction in fcc Metals: A Comparison Between Atomic Simulations and Elasticity Theory”, Acta Materialia, 54, 3543 (2006).
[5] X. Y. Liu, J. Wang and S. B. Biner, “Hydrogen and Self-Interstial Interactions with Edge Dislocations in Ni: Atomic and Elasticity Comparisons”, Modeling and Simulation in Materials Science and Engineering, 16, 045002 (2008).
[6] E. Clouet, S. Garruchet, H. Nguyen, M. Perez and C.S. Becquar, "Dislocation Interaction With C in α-Fe: a Comparison Between Atomic Simulations and Elasticity Theory", Acta Materialia, in press (2008).
[7] E. Rodary, D. Rodney, L. Proville, Y. Bréchet, and G. Martin, “Dislocation Glide in Model Ni(Al) Solid Solutions by Molecular Dynamics“, Physical Review B, 70, 054111 (2004).
[8] J. P. Hirth and L. Lothe, Theory of dislocations2nd ed, (Wiley Interscience, New York, 1982).

Influence of inertial effects on the motion and the interaction of dislocations

Laurianne Pillon, Christophe Denoual, Yves-Patrick Pellegrini

**Département de Physique Théorique et Appliquée, CEA/DAM IdF,
Bruyeres le Chatel, F-91297 Arpajon CEDEX F-91297 Arpajon CEDEX,
(E-mail : christophe.denoual@cea.fr)**

ABSTRACT

A major aspect to model strain hardening under high strain rate lies in the description of the motion and interaction of dislocations including realistic inertial effects. Up to now, equations of motion for dislocations are limited either to smooth accelerations or to small velocities, which is not sufficient to describe high strain rate. The key to describe the instationary motion of dislocations and their interactions is the retarded rearrangement of displacement fields through waves emitted by moving dislocations. On the basis of this phenomenon, we build an equation of motion for dislocations depending on a visco-inertial force [1] and on a "delayed interaction force" between dislocations. Results are compared to the one obtained with the Peierls-Nabarro Galerkin (PNG) numerical approach [2], in which no hypotheses are made about the motion and stress waves generated by moving dislocations [3]. Results are in agreement with PNG in the case of a single dislocation [1] and for a dipolar interaction. [1] Pillon L., Denoual C., Pellegrini Y-P., Equation of motion for dislocations with inertial effects, Phys. Rev. B, 76, 224105, 2007. [2] Denoual C. Dynamic dislocation modeling by combining Peierls Nabarro and Galerkin Methods, Phys.Rev. B, 70, 024106, 2004. [3] Denoual C, Modelling dislocation by coupling Peierls-Nabarro and element-free Galerkin methods, Comput. Methods Appl. Mech. Engrg., 196, 1915, 2007.